NTNU – DEPARTMENT OF CHEMICAL ENGINEERING

Biodiesel

Modelling of the production of biodiesel by reactive distillation

Emilie Øritsland Houge

07.12.2012

Specialization project Trondheim 2012.
Supervisor: Sigurd Skogestad, Co-supervisor: Chriss Grimholt

Abstract

The purpose of this project was to perform a literature search on the production of biodiesel through reactive distillation, and to create a model to describe the behaviour of this process.

A dynamic model for a reactive distillation biodiesel plant was constructed using Simulink Matlab R2012a. The biodiesel process used linoleic esters from soybean oil and methanol as the reactants with NaOH as the catalyst. It was based on design and kinetic data from the information available in the similar study of Simasatitkul et al. [1].

The liquid hydraulics were modelled by the Francis weir equation assuming constant volume holdup, while the vapour dynamics were modelled assuming constant molar overflow. The reaction rates were estimated from the rate law and assumed to only occur in the liquid phase, while a parameter that accounted for the change in composition due to reaction was added to the material balances.

The simple reactive distillation model follows the same behaviour as in the published article [1], such as number of reactive trays required, purity of biodiesel produced and temperature estimated in the column. However, the model gives slightly different results for the composition inside the column as it contains too much methanol. This is probably due to the chemical equilibrium implementation which is known to be complicated for reactive distillation processes [2]. Some further work is still required to ensure that the model is sufficient in describing the production of biodiesel through transesterification reactions in a reactive distillation column.

Acknowledgments

For the completion of this project I would like to thank my supervisor, professor Sigurd Skogestad, for his valuable insight and help. I would also like to thank my co-supervisor PhD student Chriss Grimholt for always taking the time out of his busy schedule to council me on a frequent basis and to help direct me towards the correct path in modelling.

Lastly, I would also like to thank my fellow student Marianne Øien for her collaboration on the biodiesel project, and my partners in crime at the study room: Nicola, Ketil, Ane and Vilde for keeping spirits high and making sure coffee and sugar are always available.

I hope you enjoy!

Table of Content

List of Figures

List of Tables

1. Introduction

The global energy consumption is expected to grow by 47% by 2035 [3]. Fossil fuels dominate the energy supplies by 87% while renewable energy sources only contribute with 2% to the global energy market [4]. However, liquid fuels besides petroleum are expected to triple by 2035 largely due to the projected increase in fossil fuel prices in the coming years [3]. Increasing energy demands coupled with incentives to avoid greenhouse gas emissions have contributed in making renewable energy the fastest growing energy source, expected to increase by an average of 3% per year from 2010 to 2035 [3].

Biodiesel is made from plant oils, animal fats or even waste cooking oils through transesterification and esterification reactions with alcohols. It constitutes a renewable, biodegradable and carbon neutral alternative to petroleum diesels, and can be used either on its own or in blends with regular diesel. Biodiesel can be used on most automotive engines without any modifications and can actually contribute to improving the engines' general performance [5].

The traditional process for production of biodiesel is through reactors followed by separators. However, in recent years more studies have been focusing on the prospect of using integrated reactive separation technologies in the manufacturing of biodiesel [6]. Reactive distillation is the merging of a reactor and a distillation column in one, and can offer several benefits, such as: increased yield, avoidance of azeotropes, reduced capital costs of the plant (CAPEX), more effective separation and reduced need for solvents [7].

The purpose of this specialisation project was to combine these technologies on the rise by developing a model for the production of biodiesel by reactive distillation. This model could then be used to assess the general behaviour of the system with regard to temperature profile, compositions in the column, product purity and dynamics. The behaviour of the system can then later be used to aid in design decisions and be of assistance for optimisation of process conditions and construction of control systems.

2. Background

This section is meant to provide an introduction to biodiesel and reactive distillation; the current state of the technologies and the challenges associated with them. The background is not meant to cover these subjects completely, but to provide sufficient information to understand the modelling and design decisions made, the results obtained in this report and suggestions for further work and modifications.

2.1 Biodiesel

Biodiesel is vegetable or plant-based oils that can be used as fuels, and normally consists of long chain alkyl esters. The first use of vegetable oils as fuels was demonstrated by Rudolph Diesel, the inventor of the diesel engine in the start of the 20th century. He was of the opinion that vegetable oils were the fuel of the future [5]. However, because of the cheap fossil fuel prices, biodiesel was not considered a viable alternative until recently, when fossil fuel prices have increased and are estimated to keep rising [3]. Biodiesel is promising in that it represents an environmentally friendly alternative or additive to regular fossil fuels that can be used on present engines with no or little modification. Biodiesel can also improve the performance of the engine and even prolong the engines' life as it showcases both increased solvent effect and lubrication properties [5].

Environmentally Friendly Fuel

Using biodiesel as a fuel significantly reduces harmful emissions to the atmosphere. The emissions of sulphur dioxide are reduced by 100%, while emissions of carbon monoxide, particulates and unburned hydrocarbons are reduced by 48%, 47% and 67% respectively. Also for blends of biodiesel with regular petroleum diesel, the biodiesel will improve the overall biodegradability and promote reduction of harmful emissions from the fuel [5].

One of the most important greenhouse gases is CO_2, and also here biodiesel offers an advantage: biodiesel derived from vegetable oils can be considered carbon neutral as the plant attains its carbon through absorption of carbon dioxide from the atmosphere during its lifetime. The carbon released during burning should thus be equal to the carbon previously absorbed by the plant and no excess carbon dioxide would be emitted. In total, the emissions of carbon dioxide from biodiesel are reduced by 78% from regular diesel fuels [5].

The only environmental issue with applying biodiesel as a fuel is the potential increase in NO_x emissions from fossil fuels by 6-9% in pure biodiesel. However, on-going research is exploring the possibilities of reducing these emissions with regard to changes in the injection times and temperatures of the diesel engine. The difference in formation of NO_x during combustion is most likely due to differences in the structure of the fuels, as biodiesel have a larger degree of unsaturation compared to regular fuels [5].

Challenges

One of the challenges associated with employing biodiesel as a fuel is that the source of the biodiesel in some cases often is edible and thus competes with markets for producing food for human or livestock use. Also, there is a problem with producing enough biodiesel to be able to satisfy the demands. There simply isn't enough crop space for producing biodiesel with present technology using common raw materials such as soybean oil or palm oil. To give an idea of the areas required; if all of the fats and oils produced in the US were converted to biodiesel, it would only cover 8% of the market for diesel worldwide [5].

Research has been exploring the possibilities of employing alternative sources of biodiesel with larger oil to surface area ratios required such as algae [5], or by utilising waste oils or non-edible vegetable oils that are not a source of food [6].

Soybean Oil

The number one source of biodiesel today is soybean oil (US) and palm oil [8]. Soybean oil contains a favourable energy ratio of 3 energy units produced to each energy unit consumed. However, soybean crops need large surface areas in order to grow, and hence an acre (4046 m^2) of soybean crops yields only 50 gallons (190 litres) per year [5].

The soybean consists of approximately 21% oils, whereas 94.4% is triacylglycerol and 3.7% is phospholipids. The amount of free fatty acids in the oil can vary with the age and soundness of the beans [8], but is usually quite low (less than 0.3%) [5]. The composition of the average soybean methyl ester is given in Table 2.1 below.

Table 2.1: The physical properties of the fatty acid esters of soybean oil.

Methyl ester	Chemical formula [9]	Average composition of soybean oil [8]	Boiling point [K] [9]
Linoleate	$C_{19}H_{34}O_2$	55%	619.15
Oleate	$C_{19}H_{36}O_2$	23%	617
Linolenate	$C_{19}H_{32}O_2$	7%	620.15
Palmitate	$C_{17}H_{34}O_2$	11%	597.7
Stearate	$C_{19}H_{38}O_2$	4%	623.7

Quality

The standards for biodiesel ensures that the fuel is safe to use, and reduces the possibility of it having harmful effects on the automotive engine [10]. There are separate standards for different biodiesel plants and engine manufacturers [11]. These standards are mentioned to give an idea of the purity required and the post-processing necessary to achieve a high quality product.

These standards normally contain restrictions on the amount of alcohol, free fatty acids, catalyst, unconverted soybean oil, sulphur and glycerol the biodiesel can contain. The standards also specifies acceptable values for most physical properties of the biodiesel such as cloud point, viscosity, flashpoint and many more [10]. Table 2.2 below gives an overview of some of the specifications in two standards from Europe and Germany for fatty-acid methyl ester (FAME) biodiesel [11]:

Table 2.2: The International Standards for FAME Biodiesel [11]

Specification		European standard, EN 14214:2003	German standard, DIN V 51606
Water	[mg/kg]	500 max	300 max
Total contamination	[mg/kg]	24 max	20 max
Methanol	[weight%]	0.20 max	0.30 max
Ester content	[weight%]	96.5 min	-
Monoglyceride	[weight%]	0.8 max	0.8 max
Diglyceride	[weight%]	0.2 max	0.4 max
Triglyceride	[weight%]	0.2 max	0.4 max
Free Glycerol	[weight%]	0.02 max	0.02 max
Total Glycerol	[weight%]	0.25 max	0.25 max

2.2 Production of Biodiesel

This section provides a rough overview of the processes applied for production of biodiesel, the reactions, the process conditions and emphasis of current research.

The Reaction

Oils and fats can be converted to biodiesel through either a transesterification or an esterification process with a low weight alcohol (usually methanol or ethanol) and a basic or acidic catalyst. The two different reactions are presented below [5, 12]:

Transesterification: $$TAG + 3ROH \leftrightarrow 3RCOOR' + C_3H_5(OH)_3 \quad (2.1)$$

Esterification: $$R'COOH + ROH \leftrightarrow R'COOR + H_2O \quad (2.2)$$

The transesterification reaction is the most common process for raw materials that have a low percentage of free fatty acids (FFAs), such as pure soybean oil or palm oil. The reaction raw materials consist of an alcohol reacting with a triacylglycerol (TAG) to produce glycerol and alkyl esters (the biodiesel). The process normally applies a homogeneous alkali catalyst and occurs at atmospheric pressure, modest temperatures and with an excess of alcohol present [5]. The heat of reaction is exothermic, but varies with varying composition of the biodiesel and the alcohol involved. Transesterification is a reversible reaction but in general the back-reaction does not occur as glycerol and the alkyl ester form immiscible phases [12].

The esterification reaction is used for raw materials that have a modest to high degree of free fatty acids such as waste cooking oil. This reaction converts the free fatty acids to alkyl esters in one single step, and normally employs an acid catalyst such as HCl or sulphuric acid. Because it is uncommon to have only FFAs present in a raw material source, it is normal to have the transesterification and esterification reactions occur simultaneously to target both the free fatty acids and the TAGs at the same time, or to use the esterification process as a pre-treatment step before the transesterification reaction [5].

There are two known competing reactions to the biodiesel production, called the saponification (soap-formation) reaction, and the hydrolysis reaction. These are shown below as equations 2.3 and 2.4 [5].

Saponification: $R'COOH + NaOH \leftrightarrow R'COONa + H_2O$ (2.3)

Hydrolysis: $R'COOR + H_2O \leftrightarrow R'COOH + ROH$ (2.4)

Both of these reactions are unwanted and may propose difficulties with cleaning the equipment, and dilution of the product, deactivation of the catalyst and interference with the main reaction. The saponification and hydrolysis reactions depend on the presence of free fatty acids (FFAs), but research has shown that if the amount of FFAs is less than 0.5% the reduction in reaction efficiency is negligible [12].

The Catalyst

It is most common to use homogeneous alkali catalysts for the transesterification reaction. This yields high reaction rates at low operational costs (ambient temperatures and pressures). However, the homogeneous catalyst can be difficult to recover, they cause damage to the column due to corrosive properties and waste treatment and contamination can be a challenge post-reaction [12]. The catalysts are usually present at concentrations of approximately 1 percent, and the most common catalysts are NaOH, KOH or sodium methoxide, with sodium hydroxide being the cheapest and most popular alternative. However, NaOH is also the catalyst with the highest costs associated with waste disposal, cleaning, damage to the column and also the one which has the most negative impact on the environment [5].

Research is constantly being conducted in trying to find new alternative catalysts and especially popular is the research for heterogeneous catalysts [5]. A heterogeneous catalyst reduces the number of purification steps for the biodiesel post-reaction, it is reusable, it offers an improved environmental profile [12] and it is also very beneficial for reactive distillation purposes where the catalyst can be fixed on every tray [6]. There has also been a development of processes that apply ultracritical conditions or enzymes to avoid the use of catalysts completely.

The model in this report applies a homogeneous NaOH-catalyst which for the reasons mentioned above, is not the most environmentally friendly alternative. However, the catalyst was chosen based on available kinetic data and process conditions for modelling.

The Process

There are several methods for producing biodiesel, such as batch, continuous, enzymatic, supercritical and reactive separation [6]. The advantages and disadvantages of each process are described below in Table 2.3.

Table 2.3: Overview of the different processes for producing biodiesel from methanol [6].

Process	Advantages	Disadvantages
Batch	Good flexibility with regard to feed composition.	Low productivity and high operational costs.
Continuous	Combination of transesterification and esterification reaction which leads to high productivity.	Normally uses homogeneous catalysts, which means it is subject to corrosion and extensive cleaning is necessary.
Supercritical	No catalyst and no hindrance to the transesterification kinetics due to oil-alcohol miscibility.	Severe conditions that require special equipment (costly).
Enzymatic	Low energy requirements.	Low yields and productivity, long reaction times.
Multistep	Applies both transesterification and esterification. High purity glycerol is obtained as a by-product. Solid catalyst can be used.	High capital costs
Reactive Separation	High conversion and yields, reduced post-processing	Damage of equipment if combined with homogenous catalysts

Strong incentives for efficient production of renewable fuels have shifted the interest to larger scale production of biodiesel. Because of this, the processes mostly used in industry today are the multistep and the continuous method. The enzymatic method and the supercritical method show promise but do not offer enough of an economic advantage to be applied commercially at the time being [6].

A lot of research is being developed on reactive separations at the present and this group consists of: reactive distillation, reactive absorption, membrane reactors and reactive extraction. Reactive distillation is the reactive separation process with the most applications, the focus of this paper and is explained in more detail in the next section [6].

2.3 Reactive Distillation

Integrated reactive and separation processes is not a new idea, it has been used in the petroleum industry for decades, but advances in commercial applications helped spark new interest in the technology in the 1980s. These were largely due to the successful construction of a reactive distillation process for production of methyl tert-butyl-ether (MTBE) and methyl acetate, where the latter was able to comprise a traditional process consisting of 9 distillation columns and a reactor into a single integrating column, saving a lot of money on capital costs and energy. Since then, the number of patents and research papers published on the matter has increased by tenfolds, and new applications for reactive distillation are continuously being researched [7, 13, 14].

Reactive distillation is the combination of a distillation column and a reactor in a single unit. As mentioned in the previous paragraph, the most apparent advantages are decreases in capital and operational costs. Simplified, the reactive distillation unit showcases the following characteristics as described in Table 2.4, which are categorized as advantages and disadvantages accordingly [2].

Table 2.4: Characteristics of the reactive distillation process [2]

	Advantages	Disadvantages
Continuous removal of product	- The continuous removal of products in the reaction phase shifts the equilibrium to the right and higher conversion can be achieved. - The concentration of volatile products is kept low which will reduce the rates of side-reactions and improve selectivity.	- The volatilities of the reagents and the products must be suitable in order to get the desired concentrations at desired positions in the column.
Simplification of separation system	- The elimination or reduction in separation systems gives great capital savings. - The flowsheet is simplified which leads to a simpler process which is easier to understand.	- The process conditions for the reactor and the distillation process must overlap. In some cases the conditions in the reactive distillation unit is far from optimal, and may give less efficient operation.
Heat integration	- An exothermic reaction can easily be used to supply heat of vaporisation to reduce reboiler duty. This is more efficient heat transfer than traditional heat exchangers.	
Azeotropes	- Azeotropes of the product mixture from the reactor can be avoided by reacting the mixture under specific conditions in the column.	- The presence of a reaction may introduce reactive azeotropes where there previously was none.
Liquid distribution		- Liquid distribution problems make it difficult for scale up to large flowrates.
Residence time		- A long residence time for the reaction will require a very large column with corresponding large capital costs.

On the basis of the information in Table 2.4, one can deduce that the advantage of introducing reactive distillation over the traditional reactor followed by a distillation column has the greatest potential if the process involved has limitations when it comes to conversion or separation or both. For example it is an excellent alternative for reactions with very low equilibrium rate constants and for mixtures with azeotropes [6, 13]. Often, if the process has no such problems, there is no financial benefit in changing the design to reactive distillation and it may not even be feasible [13]. E.g. the introduction of a reactive distillation column where there has previously never been any problems with separation, may introduce new “reactive azeotropes” and thus serve as a hindrance for successful separation instead of acting as a promoter. A reactive azeotrope gives a constant boiling mixture with constant liquid and vapour compositions [2, 13].

Also, it is important to note that the operational conditions for the reaction and the distillation column must overlap in order to use a combined process. A regular process that has vast differences in the limiting conditions for temperatures and pressures in the distillation column and the reactor will not yield a feasible reactive distillation process. The compromised process conditions of the

reactive distillation column may also be far from the optimum conditions of the segregated units and give worse overall performance [6].

The design of a reactive distillation column is performed in four consecutive steps: 1) determination of feasibility, 2) design of column, 3) choosing equipment and hardware and 4) optimisation and control. As this project is mainly focused on the development of a valid model, it is primarily steps 1 and 2 that will be discussed in this report [7].

Phase Equilibrium Behaviour

The phase equilibrium is normally evaluated using the residue curve map (RCM) method. The RCM method gives a graphical representation of the composition profiles for total reflux in a packed distillation column, as the light component is continuously boiled off. A simple analysis will allow one to determine whether the product should be retrieved as a distillate or as bottoms, but it also has other features; it will give information on azeotropes and possible purities that can be achieved. The stationary points on the graph are divided into three groups: unstable (all curves point outwards), stable (all curves point inwards) and saddle nodes (curves point both inwards and outwards). Azeotropes are recognized as saddle or unstable nodes and represents points where the composition remains unchanged in the vapour and liquid phase [2].

The RCM analysis for the biodiesel process is based on the presence of a tertiary system of methyl linoleate, methanol and glycerol. The tertiary system assumption was made based on the fact that the reaction goes almost to completion after a short residence time [1, 5], where the intermediate compounds, DG and MG, and the reactant TG will be present in negligible amounts. Methanol is also a reactant, but is introduced in excess amounts, and will therefore constitute a significant portion of the column compounds. The RCM analysis for the biodiesel, glycerol and methanol system is shown below in Figure 2.1 as calculated and published by Simasatitkul et al. [1].

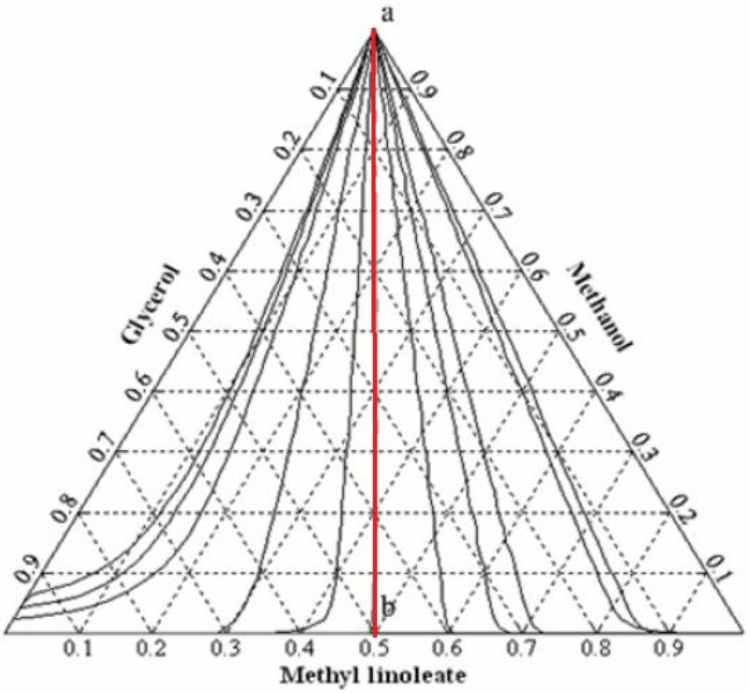

Figure 2.1: The RCM analysis of the biodiesel system of linoleate esters [1].

From Figure 2.1 one can see that the system is separated into two distillate regions by the line a-b (marked in red) which constitutes the distillate boundary. From the reaction stoichiometry it is apparent that the system will mostly be on the right hand side of the distillation boundary. Hence, as methanol is boiled off as the light component, the resulting bottom product will be a mixture of glycerol and biodiesel. A saddle azeotropes is present for the glycerol and methyl linoleate mixture, but this does not influence the process because the purpose of the reactive distillation column is not to produce pure glycerol or biodiesel but a mixture of the two and rather a "pure" methanol distillate flow.

A rough estimate of the volatilities from this diagram shows that glycerol and methyl linoleate will have low relative volatilities compared to methanol. As the boiling points of TG, DG and MG are even higher than of glycerol and biodiesel, one can assume that they will be even less volatile, and that the distillate will be almost pure methanol while the bottoms will be a mixture of heavier components.

Chemical Equilibrium Behaviour

The feasibility of the process and the product purity will depend on the production rate, the amount of catalyst and the liquid holdup as well as the volatilities. There are three methods that have been designed to account for the effects of reaction on the distillation column, also at times where reaction equilibrium is not reached (normal operating conditions for commercial processes): bifurcation theoretic methods, difference-point methods and attainable region methods. These methods will not be further explained in this report, as at the present none of these methods provide sufficient column information [13].

The behaviour of most reactive distillation systems will be an intermediate between phase equilibrium limited and reactive equilibrium limited cases. Whether the system is kinetically limited or phase limited is normally determined by the relationship between the liquid residence time and the pseudo-first order rate constant. Because of this toggle between limiting scenarios, equilibrium modelling of a reactive distillation system can be difficult [2]. However, Alejski and Duprat [15] modelled a steady-state reactive distillation column where the kinetics were accounted for by introducing a plate efficiency, appropriate kinetic equations and hydraulics. Their model compared well with experimental values.

Feasibility

The transesterification reaction is not a traditional choice for a reactive separation process as the conventional process showcases neither slow reaction kinetics nor problems with separating methanol from the glycerol/biodiesel mixture. In this case, reactive distillation is used to overcome the equilibrium limited transesterification reaction and obtaining a higher conversion and yield [1]. Reactive distillation also contributes to making a more economic process by removing some post-processing equipment, as biodiesel is produced and methanol removed in a single step [6].

As mentioned in an earlier section, the process conditions for the reactor unit and the distillation column must overlap in order for the integrated unit to be a feasible solution. For a normal transesterification process the reactor conditions are usually at ambient temperatures and pressures with an excess amount of methanol in the range of 6:1 to 20:1 for alkali catalysts. Higher temperatures can also be used as the reaction speeds up at higher temperatures and viscosity of the oils is reduced [5]. However, the temperature should not exceed 150°C or 250°C as this will lead to the decomposition of glycerol and methyl linoleate respectively [1].

The reactive distillation column will operate at the bubble point temperature of the mixture, which according to the published work of Simasatitkul et al. [1] is around 100°C. This fits well inside the specifications on the reactor. Because of the large difference in volatilities of the compounds, there is no need to operate at higher pressures; methanol is easily recovered as the light key in the distillation process.

Further Processing

To further process the biodiesel to satisfy the standards as given in Table 2.2 [11], it is required to remove excess glycerol, methanol and trace amounts of other contaminants from the product. Because of fear that the reaction may reverse, it is common practice in traditional continuous biodiesel processes to first remove the glycerol. The glycerol has little solubility in the esters and can be removed in a settling tank or a centrifuge. Some of the excess methanol is removed with the glycerol, and the rest is removed in an acid cleaning step, leaving the biodiesel in satisfaction of the biodiesel standards. The acid scrubbing (normally with sulphuric acid) is used to stabilize the pH, dissolve any soap that may have been formed from the saponification reactions and also remove some methanol. The acid cleaning step is applied for both the biodiesel and the glycerol [12, 16].

An example of a process flowsheet is shown below in Figure 2.2. This is a modification of the normal continuous process flowsheet described in the biodiesel literature [12, 16]. As little documentation has been found on the subject, it is purely a visualisation of what the transesterification reactive distillation process might look like. The largest alterations from the regular biodiesel production process are the elimination of a reactor and methanol-removal units for the glycerol and the biodiesel.

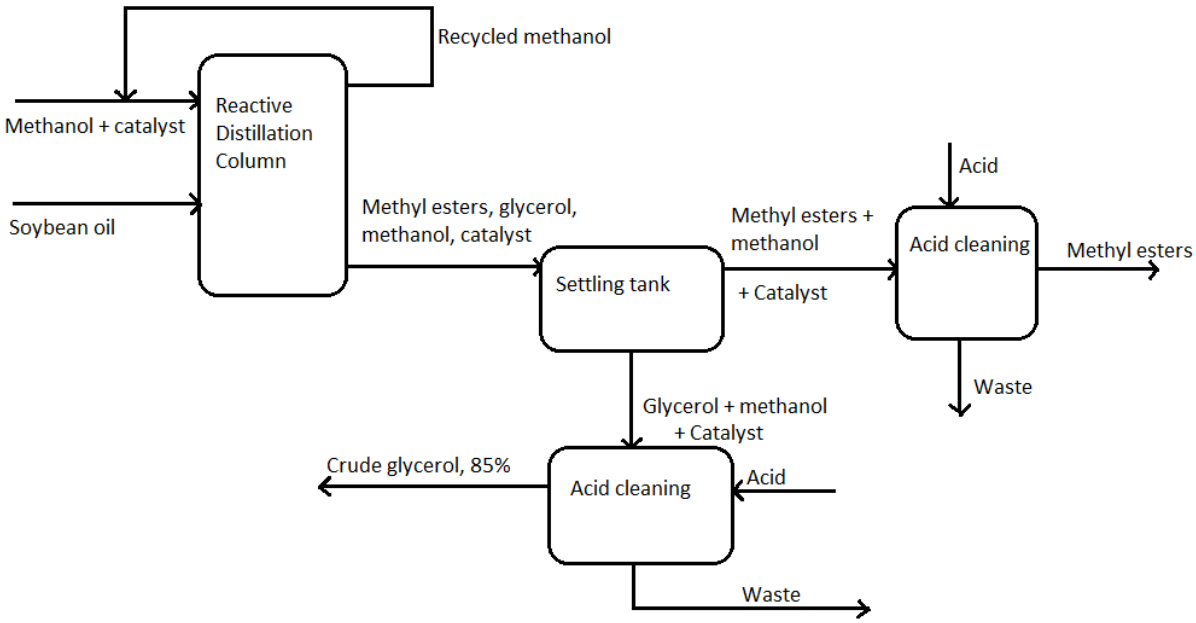

Figure 2.2: Visualised flow sheet of the reactive distillation transesterification process [12]

However, because this report is focused on the development of a dynamic model of the reactive distillation column, the report will not go into more detail of the post-processing of the biodiesel product.

3. The Basis for the Model

The model was created using Simulink, Matlab version R2012a. The model is loosely based on the distillation column for multicomponent mixture described by Skouras and Skogestad [17], and the method described in the works of Jhon and Lee[18], Rahul et al.[19] and Alejski and Duprat [15] for reactive distillation modelling. The model is a simple dynamic model which consists of molar and mass balances, liquid dynamics by the Francis weir formula, phase equilibrium by Raoult's law and kinetics by elementary kinetic equations. Energy balances have not been included.

This section gives the first of several introductions to the basic principles used in creating the model. The performance of the model is then continuously compared to the model published by Simasatitkul et al. [1] and evaluated.

The Matlab m-codes used in the project are available in appendix A, while a print of the Simulink model has been provided in Appendix B. The full Simulink model with m-codes was submitted electronically.

3.1 The Biodiesel Process

The process specified in the work by Simasatitkul et al [1], who simulated the reactive distillation production of linolein methyl-esters in Hysys Aspen-Tech was used as a basis for the model. The flowsheet of their process is shown below in Figure 3.1.

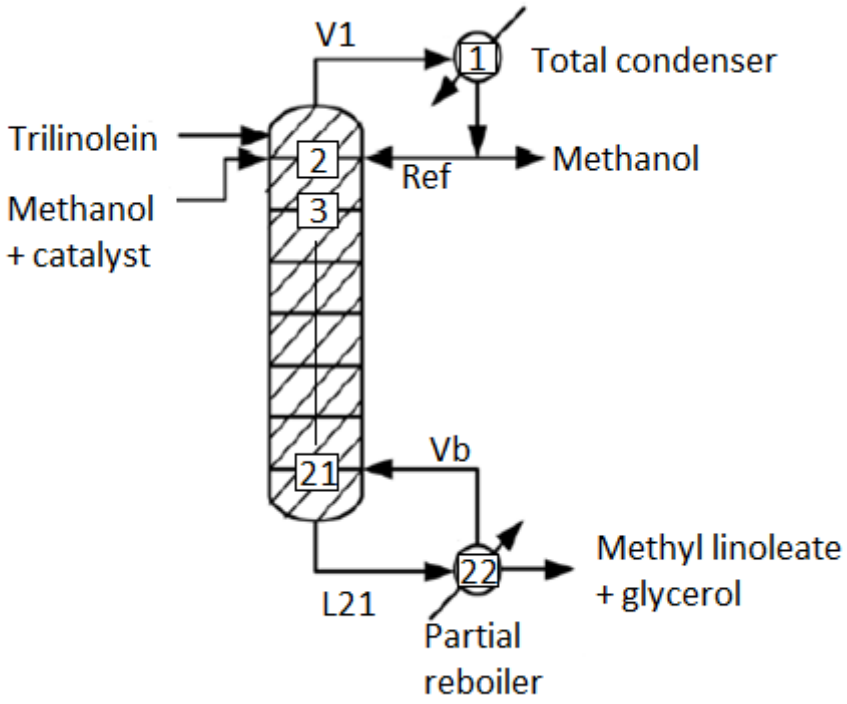

Figure 3.1: A modified flowsheet of the reactive distillation process from Simasatitkul et al. [1]

The conditions that have been applied to the model, that were specified in this report [1], are given in Table 3.1.

Table 3.1: Conditions for the reactive distillation of biodiesel from Simasatitkul et al. [1].

Condition	Value	Comment
Average temperature in the column	373.15 K	This value was used as initial values for the temperatures in the column.
Temperature of feed	323.15 K	This was the initial temperature used for the feed.
Pressure	1 atm	Atmospheric pressure was applied to the column. The pressure drop was considered negligible.
Reflux ratio	3	A reflux ratio of 3 was implemented.
Heat of reboiler	$1.2*10^7$ kJ/h	The reboiler duty was converted (roughly) to the number of moles in the vapour boilup, assuming that the vapour consists mostly of methanol this translates to approximately 430 kmol/h.
Number of trays	22	This includes the reboiler and the condenser.
Number of reactive trays	3	The number of reactive trays was calculated to be 3.
Feed tray	1	The feed is introduced at the first tray (counted from the top) because the feed contains a mixture of methanol and the catalyst. If the feed was to be introduced at a lower point in the column the number of reactive stages would be reduced as no catalyst would be present.

In addition to the applied conditions given in Table 3.1, the following assumptions were also made to ease calculations in the model:

1. The soybean oil only consists of linoleic esters.
2. The pressure drop in the column is considered negligible.
3. The rate of the saponification and hydrolysis reactions are considered negligible.
4. The course of the reactions is completely described by their kinetic equations
5. The mass of the homogeneous catalyst is negligible.
6. The catalyst will have no effect on the phase equilibrium.
7. The reaction will only occur in the liquid phase.
8. Phase equilibrium is established on every tray.
9. Chemical equilibrium is established on every tray.
10. The reaction will only occur on the actual trays and not in the reboiler or in the condenser.
11. The efficiency of the trays is 100%.
12. There is no vapour holdup.

The assumption of phase equilibrium and reactive equilibrium being established on every tray is questionable, but is a necessary assumption in order to start the modelling. The assumption of no vapour holdup is not a problem considering the low pressure of the reactive column [15].

Physical properties

Some physical and thermodynamic properties of the compounds involved in the transesterification reaction, essential for modelling are given in Table 3.2. The reported values have been collected from the DIPPR project 801 database [9] as recommended by the American Institute for Chemical Engineers (AIChE), except for the values for monolinoleate [20] and dilinoleate [21] which are not covered in the DIPPR 801 database at the present.

Table 3.2: Physical and thermodynamic properties of the biodiesel compounds [9],[21],[20]

Compound	M_w [kg/kmol]	T_b [K]	ΔH_f^0[kJ/mol]	T_c [K]	P_c [atm]	Chemical formula
Trilinoleate (TG)	879.384	895.3	-1 748	934.6	2.0004	$C_{57}H_{98}O_6$
Dilinoleate (DG)	616.9542	942.6	-	-	-	$C_{39}H_{68}O_5$
Monolinoleate (MG)	354.524	758.2	-	-	-	$C_{21}H_{38}O_4$
Glycerol (GL)	92.09383	561.0	-669.6	850.0	12.889	$C_3H_8O_3$
Methanol (MetOH)	32.04186	337.85	-239.1	512.5	79.781	CH_4O
Methyl linoleate (BD)	294.472	619.15	-605.1	767.4		$C_{19}H_{34}O_2$

Other properties such as the heat capacity (Cp_l), the heat of vaporisation (ΔH_{vap}), the density (ρ_l) and the vapour pressure (P^*) are also necessary for modelling. These properties are temperature-dependent and are described by equations 3.1-3.4.

$$\Delta H_{vap} = A[1 - T_r]^{B+CT_r+DT_r{}^2+ET_r{}^3} \quad (3.1)$$

$$Cp_l = A + BT + CT^2 + DT^3 + ET^4 \quad (3.2)$$

$$\rho_l = A/B^{\left[1+\left(1-\frac{T}{C}\right)^D\right]} \quad (3.3)$$

$$P^* = \exp\left[A + \frac{B}{T} + C \cdot \ln(T) + D \cdot T^E\right] \quad (3.4)$$

In equation 3.1 one can see that the heat of vaporization depends on the reduced temperature, which is defined below in equation 3.5:

$$T_r = \frac{T}{T_c} \quad (3.5)$$

The parameters for these equations are also from the DIPPR 801 database and are given in Table 3.3 below. Table 3.3 only contains data for MetOH, TG, BD and GL [9], while temperature-dependent data for DG and MG are presented in the next section.

Table 3.3: Temperature Dependent Properties of TG, GL, MetOH and BD [9]

	Cp_l [J/kmol*K]	ΔH_{vap} [J/kmol]	ρ_l[kmol/m^3]	P^* [Pa]
TG	$A = 9.2969 \cdot 10^5$ $B = 2.6920 \cdot 10^3$ $C = -4.4542 \cdot 10^{-1}$	$A = 2.8206 \cdot 10^8$ $B = 5.2602 \cdot 10^{-1}$ $C = 5.8539 \cdot 10^{-1}$ $D = -7.7286 \cdot 10^{-1}$	$A = 2.6085 \cdot 10^{-2}$ $B = 1.4259 \cdot 10^{-1}$ $C = 9.346 \cdot 10^2$ $D = 2.8571 \cdot 10^{-1}$	$A = 2.3471 \cdot 10^2$ $B = -3.4699 \cdot 10^4$ $C = -27.250$ $D = 1.5475 \cdot 10^{-18}$ $E = 6$
GL	$A = 7.8468 \cdot 10^4$ $B = 4.8071 \cdot 10^2$	$A = 1.1067 \cdot 10^8$ $B = 4.8319 \cdot 10^{-1}$	$A = 9.2382 \cdot 10^{-1}$ $B = 2.4386 \cdot 10^{-1}$ $C = 8.5000 \cdot 10^2$ $D = 2.2114 \cdot 10^{-1}$	$A = 99.986$ $B = -1.3808 \cdot 10^4$ $C = -10.088$ $D = 3.5712 \cdot 10^{-19}$ $E = 6$
MetOH	$A = 2.5604 \cdot 10^5$ $B = -2.7414 \cdot 10^3$ $C = 1.4777 \cdot 10^1$ $D = -3.5078 \cdot 10^{-2}$ $E = 3.2719 \cdot 10^{-5}$	$A = 5.0451 \cdot 10^7$ $B = 3.3594 \cdot 10^{-1}$	$A = 2.3267$ $B = 2.7073 \cdot 10^{-1}$ $C = 5.1250 \cdot 10^2$ $D = 2.4713 \cdot 10^{-1}$	$A = 82.718$ $B = -6.9045 \cdot 10^3$ $C = -8.8622$ $D = 7.4664 \cdot 10^{-6}$ $E = 2$
BD	$A = 2.2999 \cdot 10^5$ $B = 9.9221 \cdot 10^2$ $C = 6.7574 \cdot 10^{-3}$	$A = 1.2934 \cdot 10^8$ $B = 9.5883 \cdot 10^{-1}$ $C = -8.7844 \cdot 10^{-1}$ $D = 2.8268 \cdot 10^{-1}$	$A = 2.0469 \cdot 10^{-1}$ $B = 2.3737 \cdot 10^{-1}$ $C = 7.6740 \cdot 10^2$ $D = 2.8571 \cdot 10^{-1}$	$A = 1.0547 \cdot 10^2$ $B = -1.4531 \cdot 10^4$ $C = -10.98$ $D = 2.5753 \cdot 10^{-18}$ $E = 6$

Estimations for DG and MG

The vapour pressure and liquid density equations for DG and MG had to be estimated, as they were not described in any available database. The vapour pressure estimations applied Reidels method which is based on the critical temperatures and pressures of the compound. The estimation method applies to the same equation as for the DIPPR 801-derived parameters [22].

The critical temperatures and pressures for MG and DG also had to be estimated. Various methods are available for this purpose with varying degrees of validity and difficulty. For this project, the Joback method was chosen. The critical temperatures and pressures calculated are given in Table 3.4, along with the calculated parameters of the vapour pressure equation. More information along with detailed calculations on the Joback method and the Reidel method is available in Appendix C and Appendix D respectively.

Because of the large uncertainties associated with parameter estimations by group contribution methods, the liquid density-equations estimation for DG and MG took a simpler approach; and were estimated as intermediate values of the densities of TG and BD. These equations are also shown in Table 3.4.

Table 3.4: Temperature dependent propeties for DG and MG

	T_c [K]	P_c [MPa]	P^* [Pa]	ρ_l[kmol/m^3]
DG	1327.79	0.46368	$A = -15.931$ $B = -2111.0$ $C = 2.4303$ $D = 8.0567 \cdot 10^{-21}$ $E = 6$	$\frac{2}{3}\rho_l[TG] + \frac{1}{3}\rho_l[BD]$
MG	932.43	1.1625	$A = 118.95$ $B = -20181$ $C = -14.318$ $D = 9.1481 \cdot 10^{-19}$ $E = 6$	$\frac{1}{3}\rho_l[TG] + \frac{2}{3}\rho_l[BD]$

3.2 The Reactions

The model is focused on the main ester of soybean oil, trilinolein. Trilinolein will react to form biodiesel through the transesterification reaction. The consecutive steps of the transesterification reaction are given below as reactions 3.6-3.8 [5].

$$TG + CH_3OH \overset{k_1,k_2}{\longleftrightarrow} DG + RCOOCH_3 \quad (3.6)$$

$$DG + CH_3OH \overset{k_3,k_4}{\longleftrightarrow} MG + RCOOCH_3 \quad (3.7)$$

$$MG + CH_3OH \overset{k_5,k_6}{\longleftrightarrow} GL + RCOOCH_3 \quad (3.8)$$

Here the first rate constant for each reaction constitutes the rate constant for the forward reaction while the latter represents the rate constant for the reverse reaction. The values for the rate constants and the activation energies of the reactions 3.6-3.8 are given in Table 3.5, in the form of the Arrhenius Equation which is displayed below as equation 3.9 [23].

$$k_i = A_i \cdot exp\left\{\frac{Ea_i}{RT}\right\} \quad (3.9)$$

Table 3.5: The kinetic parameters for the transesterification reactions [1]

Rate constant	A [m^3 kmol^{-1} h^{-1}]	E_a [kJ mol^{-1}]
k_1	$1.4040 \cdot 10^{11}$	54.999
k_2	$2.0808 \cdot 10^{9}$	41.555
k_3	$2.1262 \cdot 10^{16}$	83.094
k_4	$3.5597 \cdot 10^{13}$	61.250
k_5	$1.9206 \cdot 10^{7}$	26.865
k_6	$7.5600 \cdot 10^{7}$	40.116

The equations for the rate of change per species are shown below, developed from the rate law [23].

$$r_{TG} = -k_1[TG][MetOH] + k_2[DG][BD] \quad (3.10)$$

$$r_{DG} = k_1[TG][MetOH] - k_2[DG][BD] - k_3[DG][MetOH] + k_4[MG][BD] \quad (3.11)$$

$$r_{MG} = k_3[DG][MetOH] - k_4[MG][BD] - k_5[MG][MetOH] + k_6[BD][GL] \quad (3.12)$$

$$r_{GL} = k_5[MG][MetOH] - k_6[BD][GL] \quad (3.13)$$

$$r_{MetOH} = -k_1[TG][MetOH] + k_2[DG][BD] - k_3[DG][MetOH] + k_4[MG][BD] - k_5[MG][MetOH] + k_6[BD][GL] \quad (3.14)$$

3.3 The Distillation Column

The distillation column was developed using the multicomponent column A model by Skouras [17] as the template. To model a distillation column it is necessary to include material balances, liquid dynamics and the vapour phase equilibrium. A visualisation of the column was shown previously in Figure 3.1, where the stages are numbered from top to bottom. The feed is introduced at stage 2 (with the condenser drum as stage 1).

The inputs to the distillation column are the feed and the feed composition. The manipulated variables consist of the vapour boilup (Vb), the reflux (Ref), the bottoms product flowrate (B) and the distillate flowrate (D).

There are 6*22 available degrees of freedom in the column. It is desirable to calculate both the total molar holdup and the molar fractions on each tray. Therefore it was decided to use the molar fractions of 5 of the components and the molar holdup at every stage as the states in the iteration. This way, the molar composition of the last component was found by overall mass balances.

Material Balances

Because the column is also a reactor, the number of moles is changing, and hence the molar balances must only be applied in the sections where it is assumed to be no reaction. This will constitute the reboiler and the condenser, whose molar flows are shown below in equations 3.15 and 3.16.

$$V_1 = Ref + D \quad (3.15)$$

$$L_{Ntrays+1} = B + Vb \quad (3.16)$$

Also, the first liquid flowrate and the last vapour flowrate are set by the reflux and the vapour boilup accordingly:

$$L_1 = Ref \quad (3.17)$$

$$V_{Ntrays+1} = Vb \quad (3.18)$$

The total molar holdup and the individual molar holdup for unreactive trays in the column are given below:

$$\frac{dHR_j}{dt} = V_j - V_{j-1} + L_{j-1} - L_j \quad (3.19)$$

$$\frac{dHR_j x_{i,j}}{dt} = V_j y_{i,j} - V_{j-1} y_{i,j-1} + L_{j-1} x_{i,j-1} - L_j x_{i,j} \quad (3.20)$$

In the reactive parts of the column there is also a requirement for balances, and molar balances were applied for simplicity and consistency. To correct for the change in moles due to reactions occurring,

an extra parameter was added ($M_{i,j}$). The reactive parameter is defined below, where the value VR_i represents the volume holdup of component i [23]:

$$M_{i,j} = r_{i,j} \cdot VR_{i,j} \qquad (3.21)$$

$$M_j = \sum_{i=1}^{NC} r_{i,j} \cdot VR_{i,j} \qquad (3.22)$$

The resulting balances for the total molar holdup and the individual molar holdup on the reactive trays are shown below as equations 3.23 and 3.24.

$$\frac{dHR_j}{dt} = V_j - V_{j-1} + L_{j-1} - L_j + M_j \qquad (3.23)$$

$$\frac{dHR_j x_{i,j}}{dt} = V_j y_{i,j} - V_{j-1} y_{i,j-1} + L_{j-1} x_{i,j-1} - L_j x_{i,j} + M_{i,j} \qquad (3.24)$$

On the feed tray, the molar balance must also account for the additional feed molar flowrate. The subscript F is used to indicate that this balance is only for the feed tray.

$$\frac{dHR_F}{dt} = V_F - V_{F-1} + L_{F-1} - L_F + M_F + F \qquad (3.25)$$

$$\frac{dHR_F x_{i,F}}{dt} = V_F y_{i,F} - V_{F-1} y_{i,F-1} + L_{F-1} x_{i,F-1} - L_F x_{i,F} + M_{i,F} + F x_{i,F} \qquad (3.26)$$

The individual molar holdup differential can be rewritten in terms of the derivatives of the composition with time and the derivative of the total molar holdup:

$$\frac{dHRx}{dt} = HR\frac{dx}{dt} + x\frac{dHR}{dt} \qquad (3.27)$$

To find the change in molar fraction with time, (dx/dt), from the change in individual molar holdup with time ($dHRx/dt$), algebraic manipulation of equation 3.27 yields:

$$\frac{dx}{dt} = \frac{\frac{dHRx}{dt} - x\frac{dHR}{dt}}{HR} \qquad (3.28)$$

Vapour Equilibrium

Raoult's law is an ideal law that describes vapour-liquid phase-behaviour at equilibrium. The law is cited in equations 3.29-3.30 which give relations for the vapour (y_i) and liquid (x_i) compositions in regard to the vapour pressure (P_i^*) exerted by the liquid in a binary mixture [24]:

$$P = x_i P_i^* + x_j P_j^* \qquad (3.29)$$

$$y_i = \frac{x_i P_i^*}{P} \qquad (3.30)$$

Equation 3.29 can easily be extended to cover multiple component mixtures. However it is common to simplify calculations by introducing a general parameter such as the relative volatility. The relative volatility is a measure for how volatile the compounds are compared to a reference compound. The equations are shown below for a reference compound c [25]:

$$\alpha_i = \frac{y_i/x_i}{y_c/x_c} \qquad (3.31)$$

$$y_i = \frac{\alpha_i \cdot x_i}{\sum_{i=1}^{NC} \alpha_i \cdot x_i} \quad (3.32)$$

A very rough estimation of the relative volatilities for the process was performed by considering the respective boiling points of the compounds, with methanol as the reference compound:

$$\alpha = [\alpha_{MetOH} \quad \alpha_{TG} \quad \alpha_{DG} \quad \alpha_{MG} \quad \alpha_{GL} \quad \alpha_{BD}]$$

$$\alpha = [1 \quad 0.01 \quad 0.01 \quad 0.02 \quad 0.05 \quad 0.03]$$

However, these correlations are only valid for ideal systems such as benzene-toluene. Even for ideal systems, the relative volatility will change with varying temperatures, and for non-ideal systems they may also change with composition [24].

To correct for non-ideality a parameter called the liquid phase activity coefficient γ_i is introduced, which has to do with how the compounds behave towards each other in the liquid phase and whether the combined vapour pressure will be higher or lower than the ideal [25]. The liquid phase activity coefficient can be estimated by application of thermodynamic methods such as UNIFAC/UNIQUAC. These methods are extensive and time consuming and because of time-constraints, this method was not implemented in the dynamic model. The vapour phase equation with γ_i is shown in equation 3.33 below for low pressure systems [26]:

$$y_i P = \gamma_i x_i P_i^* \quad (3.33)$$

3.4 Results – The Column Profile

The column profile in terms of mass fractions in the liquid phase is shown below in Figures 3.2 and 3.3 for the application of Raoult's law and relative volatilities in calculation of the vapour equilibrium. These values are compared to the results obtained by Simasatitkul et al. displayed in Figure 3.4 which applied the UNIQUAC thermodynamic model [1]. The mass fractions of the three main components; MetOH, GL and BD are also summarised in Table 3.6 below.

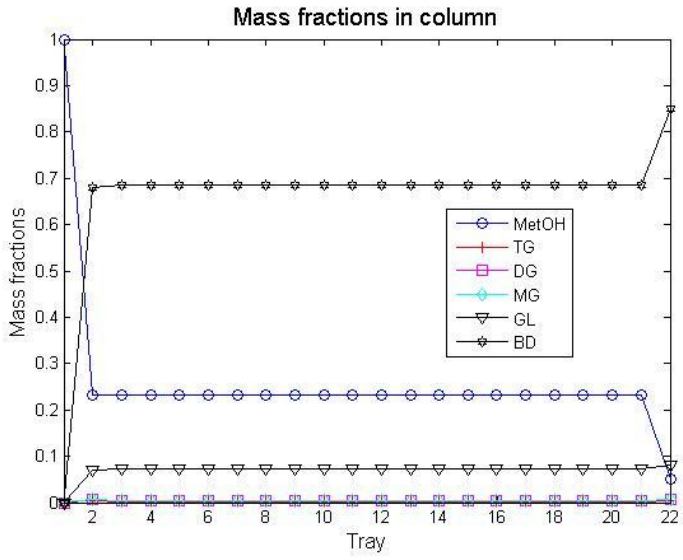

Figure 3.2: The mass fractions in the column simulated using relative volatilities

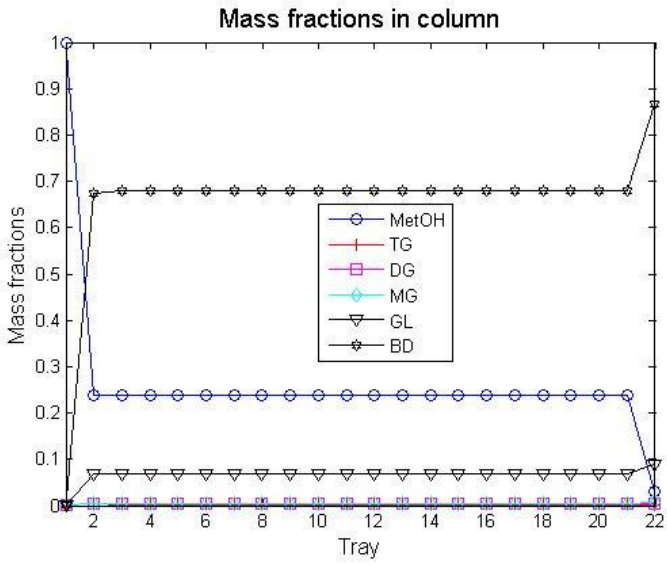

Figure 3.3: The mass fractions in the column simulated using Raoult's law

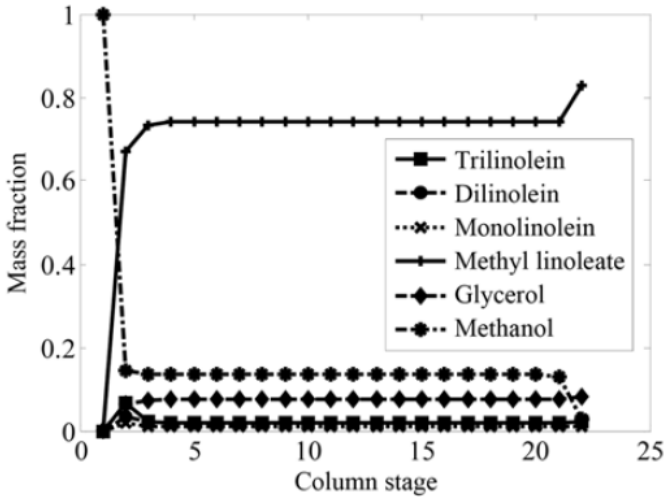

Figure 3.4: The reactive distillation column profile for mass fractions from literature [1].

Table 3.6: The mass fractions of MetOH, GL and BD for the three different models

	Relative volatilities			**Raoult's law**			**Literature values ±0.02**		
	$x_{w,MetOH}$	$x_{w,GL}$	$x_{w,BD}$	$x_{w,MetOH}$	$x_{w,GL}$	$x_{w,BD}$	$x_{w,MetOH}$	$x_{w,GL}$	$x_{w,BD}$
Tray 1	1.0000	0.0000	0.0000	0.9999	0.0000	0.0000	1.00	0.00	0.00
Tray 2	0.2317	0.0682	0.6804	0.2392	0.0691	0.6753	0.16	0.05	0.67
Tray 10	0.2312	0.0688	0.6846	0.2387	0.0698	0.6799	0.15	0.08	0.76
Tray 22	0.0519	0.0792	0.8500	0.0301	0.0890	0.8662	0.04	0.09	0.84

Comments

There are some differences in the simulation results compared to the work published by Simasatitkul et al [1]. The main deviation is that the mass fraction of methanol in the column is higher in the simulation than in the published results. The difference observed could be due to non-ideality of the

system, not reaching chemical equilibrium or differences in the implementations of the kinetics in the Simulink model compared to the Hysys model.

There is a slight peak in the intermediate components in the published results around stage 2, which is not visible in the simulated results. However, this peak is also present in the simulations, but is much smaller. This might be due to the excess amounts of methanol being present in the column which dilutes the liquid compositions, and also differences in the chemical equilibrium implementations.

On the other hand, the simulated graphs using the relative volatility and Raoult's law are very similar. This demonstrates that implementation of Raoult's law may not be necessary, as a rough estimate of the relative volatilities using the boiling points gave almost the same result. The relative volatilities also have the benefit that they can be tuned to give an even better performance of the model. The tuning at this point is not optimal, but this represents an example of further work required for the model to function properly. Because the tuning at this point is not optimal, Raoult's law is used for the remainder of the project as it better describes the system when subject to disturbances.

The product purity of the Simulink model is higher than the literature values, which would mean less post-processing if they would prove to be valid. This means that it would probably be sufficient to introduce acid scrubbing and a settling tank for glycerol removal to obtain biodiesel of European/German standard.

It is also clear from both the simulation and the literature values that the number of trays can be greatly reduced. The reaction occurs mainly on the first three stages, and the liquid composition after that remains constant until it reaches the reboiler. This is approximately the same result that Simasatitkul et al. achieved, and is a confirmation of fast kinetics of the transesterification reaction. The number of stages is not reduced, even though most of them are redundant; in order to better compare the results of the model simulation with the literature values.

Alternative Implementation of Kinetics

In the report of Simasatitkul et al. the rate equations given differ slightly from the standard equations derived from the rate law. The published equations for change in concentration with time for TG and MG are shown in equations 3.34 and 3.35 respectively. The change from the rate law is indicated by a red colour.

$$r_{TG} = -k_1[TG][MetOH] + k_2[DG][\mathit{MetOH}] \quad (3.34)$$

$$r_{MG} = k_3[DG][MetOH] - k_4[MG][\mathit{MetOH}] - k_5[MG][MetOH] + k_6[BD][GL] \quad (3.35)$$

During the course of this work this difference was considered a misprint. However, the excess amount of methanol in the column gave room for suspicion and this was investigated. The implementation of the rate equations described by equations 3.34 and 3.35 is shown in Figure 3.5.

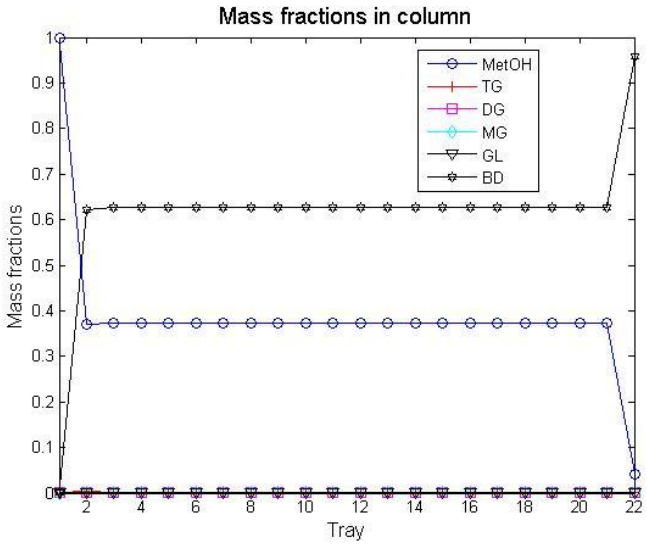

Figure 3.5: Mass fractions with rate equations as published by Simasatitkul et al.[1]

From Figure 3.5 one can see that the glycerol concentration is almost zero which is not consistent with the reaction stoichiometry, methanol mass fractions have increased even more in the column, and the product achieved is almost pure biodiesel. This implementation clearly did not improve the model performance with regard to published results.

4. Fluid Dynamics

This section describes how the fluid dynamics for the liquid and the vapour phase were implemented and gives a brief introduction to the Francis' weir equation. The section ends with a comparison of dynamics with a regular distillation column and the effect of introducing disturbances in the feed.

4.1 Liquid Dynamics

For the liquid dynamics, an adaptation of the Francis' weir formula was applied which calculates the liquid crest over the weir (h_{ow}) as an equation of the weir length (l_w), the density of the liquid (ρ_L) and the liquid flowrate (L_w) [27]. The equation for the liquid flow from each tray was derived and is shown below as function 4.1.

$$L_w = \left[\frac{h_{ow} \cdot 10^{-3}}{750}\right]^{1.5} \cdot \rho_L \cdot l_w \qquad (4.1)$$

The Francis weir equation is further illustrated in Figure 4.1 which shows the flow behaviour of the liquid on a rectangular tray in a distillation column.

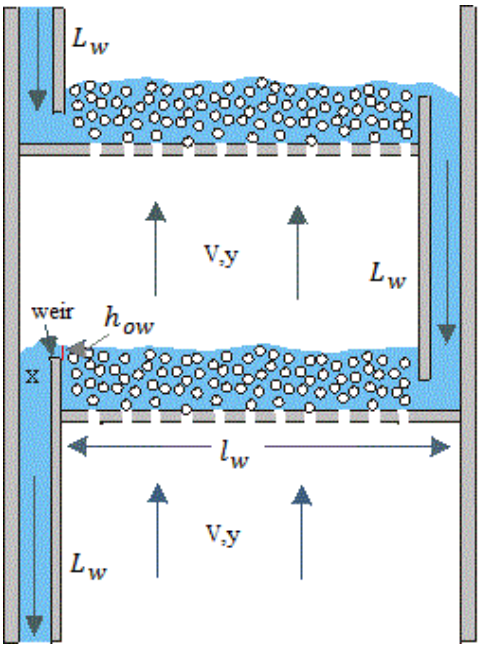

Figure 4.1: A visualisation of the vapour and liquid dynamics [28]

The diameter of the column depends on the vapour and liquid flowrates. To ensure a high efficiency, one should have a high vapour velocity, typically in the range of 80-85% of flooding velocity. The flooding velocity is calculated by applying equation 4.2 below [27]:

$$u_f = K_1\sqrt{\frac{\rho_L - \rho_V}{\rho_V}} \qquad (4.2)$$

The constant $K_1$is dependent on the tray spacing applied and is usually found from available graphs of K_1 plotted against F_{LV} for various values of the tray spacing. The tray spacing typically varies with the size of the column and is usually a value between 0.15 and 1m. The value used for this column was an intermediate of 0.45m. The equation for F_{LV} is given below [27]:

$$F_{LV} = \frac{L_w}{V_w}\sqrt{\frac{\rho_V}{\rho_L}} \qquad (4.3)$$

The diameter of the column, which equals the length of the weir, is estimated using equation 4.4 from the total column cross-sectional area (A_c) [27]:

$$D_c = \sqrt{\frac{4 \cdot A_c}{\pi}} \qquad (4.4)$$

The weir length should be approximately 0.77 of the column diameter, which can be found from application of equation 4.4. The weir itself is normally between 40-90mm high, with a recommended value of 40-50mm for regular distillation [27]. Because it is desirable to have a larger holdup on the weirs to account for the reactions and give larger residence times [7], the weirs are chosen to have a height of 200mm. The h_{ow}should be no less than 10mm to ensure even flow of liquids [27], and can be calculated from equation 4.5 where HR_i is the molar holdup on each tray. Foaming is assumed to be negligible, and the tray is assumed to have a constant volumetric holdup:

$$h_{ow,i} = \frac{HR_i - \pi \cdot 0.88\left(\frac{D_c}{2}\right)^2 h_w \rho_l}{\pi \cdot 0.88\left(\frac{D_c}{2}\right)^2 \rho_l} \qquad (4.5)$$

To avoid getting negative liquid flowrates due to the holdup on the tray being less than the weir height, a specification was added which sets the flowrate equal to zero in this case. The detailed calculations for the Francis weir parameters are available in Appendix E.

4.2 Vapour Dynamics

For the vapour dynamics, constant molar flowrate was assumed. As earlier discussed, the pressure in the column is low, so this is likely a viable assumption. This means that the flowrate set by the vapour boilup in the reboiler equals the flowrate throughout the rest of the column (equation 4.6):

$$V_j = Vb \qquad (4.6)$$

A correction had to be made for the feed tray. Here, an extra flow of unsaturated liquid is introduced, which reduces the vapour flowrate. The vapour flowrate above the feedtray is hence defined by equation 4.7:

$$V_{F-1} = V_F + (1 - q)F \qquad (4.7)$$

4.3 Feed Liquid Fraction

The feed to the column is cold liquid, so it was necessary to calculate the parameter q, which is an estimate for "..the number of moles of saturated liquid produced on the feed plate by each mole of feed added to the tower"[24]. The parameter q was calculated by applying equation 4.8 below:

$$q = \frac{H_V - H_F}{H_V - H_L} \qquad (4.8)$$

From equation 4.8 one can see that q depends on the enthalpies of the feed at dew point (H_V), bubble point (H_L) and at the feed conditions (H_F) [24]. The bubble and dew point temperatures were found by iterations applying Raoult's law, while the enthalpies were calculated from the enthalpies of formation, enthalpies of condensation and the liquid heat capacity according to Hess' law [29]. For more information on the calculations and the methods applied see Appendix F, all parameters required were provided by the DIPPR project 801 database [9].

From its definition, the feed liquid fraction is dependent on the temperature. Later on, it is desirable to look at different values for the feed temperature and hence selected values are reported below in Table 4.1:

Table 4.1: Values of q at different feed temperatures

Temperature [K]	Feed liquid fraction
298.15	1.064
303.15	1.057
313.15	1.043
323.15	1.028
333.15	1.013
343.15	0.998
353.15	0.982

4.4 Level Controllers

To ensure that the levels of the condenser and reboiler are kept stable (avoiding drift), two level controllers were installed. The configuration chosen was standard: the reboiler level was coupled with the bottoms flowrate while the condenser level was coupled with the distillate flowrate [30]. The controllers were both simple P-controllers with a gain of negative 10. The set points for the reboiler and the condenser levels were set to 100 kmol, to ensure a large buffer with regard to disturbances.

The complete Simulink model with the controller configuration is available in Appendix B as a print while the dynamic model has been submitted electronically.

4.5. Results – Dynamics

This section evaluates the dynamic of the reactive distillation column, both to ensure that the flowrates are reasonable, and to evaluate the columns performance when disturbances in the flowrate are introduced.

Dynamic Evaluation

The column dynamics were compared to the dynamics of the multicomponent distillation column model Column A by Skouras [17] to ensure that they were reasonable. The values for Column A and the reactive distillation column are shown in Table 4.2 below:

Table 4.2: Comparison of Dynamics

	Column A	Reactive Distillation
Liquid flowrate over feed (L_{of})	162.4 kmol/h	315.15 kmol/h
Liquid flowrate below feed (L_{bf})	222.4 kmol/h	674.95 kmol/h
Vapour flowrate over feed (V_{of})	192.4 kmol/h	420.20 kmol/h
Vapour flowrate below feed (V_{bf})	192.4 kmol/h	430.00 kmol/h
Feed flowrate (F)	60 kmol/h	350.0 kmol/h
Holdup Condenser (HR_{con})	0.5 kmol	100.0 kmol
Holdup Tray (HR_{tray})	0.5 kmol	8.32 kmol
Holdup Reboiler (HR_{reb})	0.5 kmol	100.0 kmol
L_{of}/V_{of}	$\frac{162.4}{192.4} = 0.84$	$\frac{315.15}{420.20} = 0.75$
L_{bf}/V_{bf}	$\frac{222.4}{192.4} = 1.16$	$\frac{674.95}{430.00} = 1.57$
F/HR_{tray}	$\frac{60}{0.5} = 120$	$\frac{350}{8.32} = 42.07$
L_{bf}/HR_{tray}	$\frac{222.4}{0.5} = 444.8$	$\frac{674.95}{8.32} = 81.12$
V_1/HR_{con}	$\frac{192.4}{0.5} = 384.8$	$\frac{420.20}{100} = 4.20$
L_{NT+1}/HR_{reb}	$\frac{222.4}{0.5} = 444.8$	$\frac{674.95}{100} = 6.75$

From Table 4.2 one can see some differences between the reactive distillation model and the multicomponent model by Skouras. The largest difference is in the size of the holdups compared to the flowrates. The holdups for the reactive distillation column were designed to be larger than normal because it was desired to have increased residence time for the reaction. This result was therefore expected. The holdups in the condenser and the reboiler are also very large compared to Column A (although it is mentioned in the code of column A that these holdups are very small). The holdups act as buffers to the system should any disturbances occur, but a very large volume will consume a lot of energy and the capital costs will increase. The holdups of the condenser and reboiler are therefore decreased by a factor of 4 to 25 kmol from hereon.

The ratios between liquid and vapour flowrates are quite similar, both above and below the feed. The reactive distillation model has more vapour compared to liquid flowrate above the feed, which is due to the reflux ratio specified. While below the feed, the reactive distillation column has slightly more liquid flow than vapour, which is due to the vapour boilup specified.

4.6 Effect of Disturbances in Flowrate

A disturbance in the flowrate was introduced to see how the process would react. Because the liquid feed fraction is more than 1, the liquid flowrate is sensitive to changes in the feed flowrate. This requires the use of solver ode23s, as ode15s cannot handle the sudden surge/drop. The relative tolerance also had to be relaxed to a value of 10^{-5} in order for the simulation to run. One should be aware that the process runs slowly when large disturbances occur.

Effect on Dynamics

Below is a figure of the liquid and vapour dynamics at various positions in the column with a +10% step change in the feed molar flow.

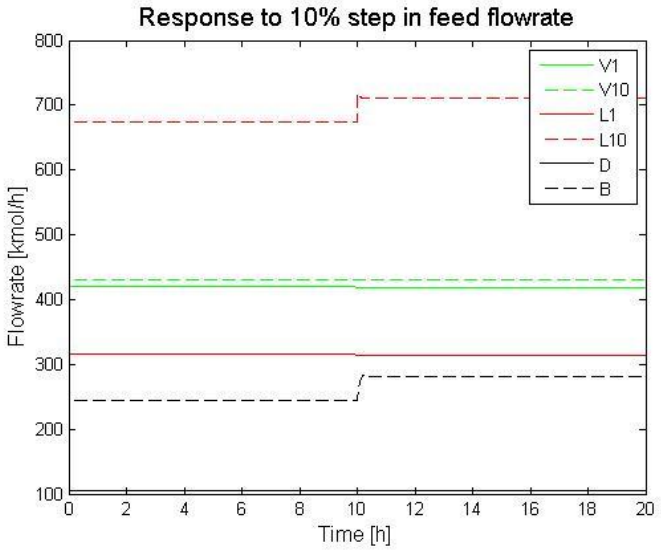

Figure 4.2: The dynamic response to a +10% step change in the feed flowrate

From Figure 4.2 one can see that the system responds as expected; an increase in the feed flowrate results in an increase of the liquid flowrate, while the vapour flowrate is hardly affected. The vapour boilup is not affected at all because it is set as a constant value. In reality the vapour boilup is determined by the amount of energy put into the reboiler. If the amount of energy is kept constant, the vapour boilup would actually decrease because more liquid is flowing through the reboiler, which would increase the amount of methanol present in the product. A higher mass fraction of methanol in the product could potentially lead to problems with reaching quality standards for biodiesel.

Effect on the molar composition

As mentioned in the last section, a disturbance in the feed flowrate will also affect the column composition profile. The effect is shown below in Figure 4.3 for the three major components; methanol, biodiesel and glycerol as molar fractions in three different positions in the column with time.

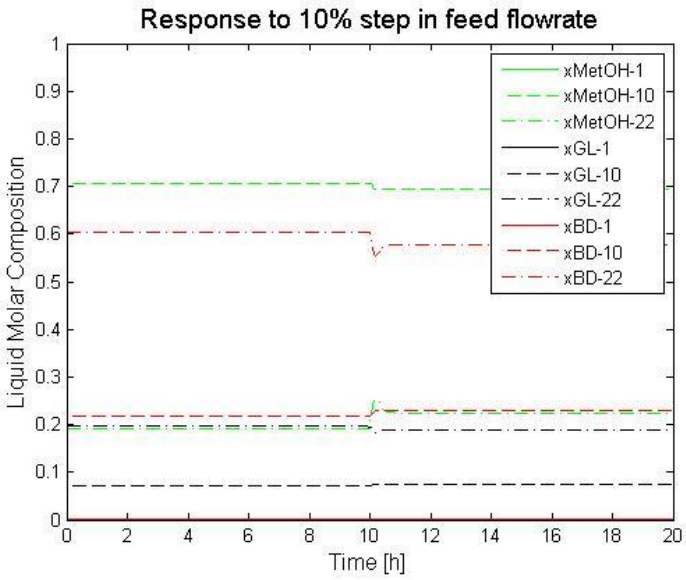

Figure 4.3: The molar compositions of MetOH, GL and BD after +10% step change in the feed flowrate

From Figure 4.3 one can see that the molar fractions in the condenser are influenced quite a lot by the change in the molar flowrate of the feed. In the product, methanol content increases while biodiesel and glycerol decrease. However, in the main part of the column the effect is not as large; the methanol molar fraction decreases while glycerol and biodiesel increase.

4.7 Effect of Disturbances in Feed Composition

To evaluate how the process would react to disturbances in the feed composition, a step change was introduced which went from a feed containing [300 50] kmol of MetOH and TG respectively to [290 60]. The results are shown below in Figures 4.4 and 4.5 for the flowrates and the moar fractions respectively. The change in the feed liquid fraction has been disregarded for this example. Calculating a new value for q would require calculation of a new boiling point and dew points and new enthalpies at the feed, dew point and boiling point.

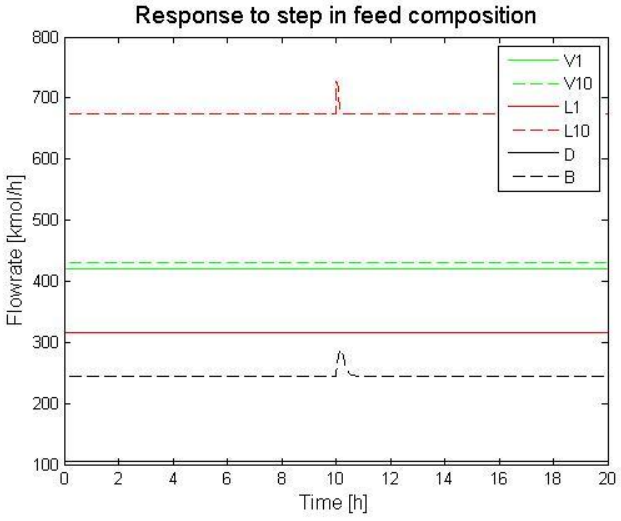

Figure 4.4: The effect of step change in feed composition on the dynamics

From Figure 4.4 one can see that the step change in feed composition leads to a fast and large surge in the liquid flowrate and a smaller surge in the bottoms, but this is quickly stabilized and returned to steadystate. This is probably due to the decreased molar holdups in the column because of the increased molar density of the mixture with increased composition of TG in the feed.

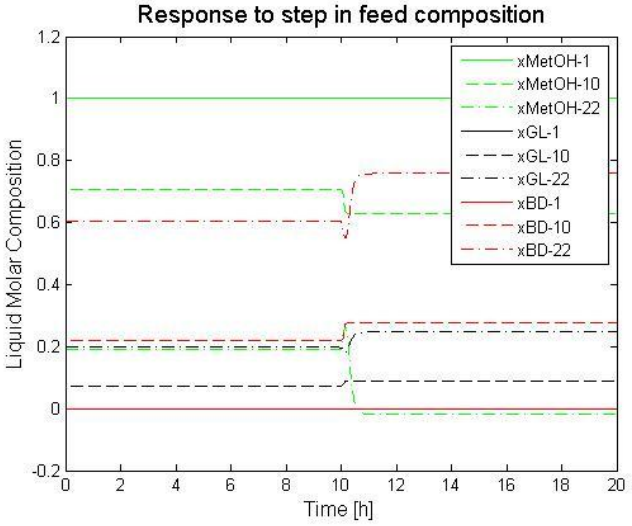

Figure 4.5: The effect of step change in the feed composition on the molar fractions

The change in feed molar fractions has the largest impact on the bottom composition in the liquid phase. Methanol decreases a lot, while biodiesel and glycerol increase slightly. The methanol actually gives a slightly negative molar flowrate in the bottoms (-0.002 mass fraction), which is not a physically feasible solution. When the solution is not feasible it is difficult to say how the process would behave in real life to this disturbance, but it seems safe to say that it would have a large effect. A constraint should be configured to keep the compositions and flowrates from turning negative, and the model should be investigated for other errors in the chemical equilibrium implementation.

The liquid composition in the column is not subject to as large of a change, but the fraction of methanol decreases while the fraction of glycerol and biodiesel increases. The composition in the condenser has an increase of all components except for methanol. However, methanol is still strongly dominant, and thus the change is not visible in Figure 4.5.

5. Temperature Estimations

Energy balances were not included in the dynamic model and because of this the temperature had to be estimated using alternative methods. This section covers the theory of the different estimation methods applied and how the theories perform compared to literature values.

5.1 Estimation Theories

Three different methods were applied for the calculation of the temperatures in the reactive distillation column. They are explained in more detail below.

Method 1: Simple Boiling Point

The first temperature estimation method used in the Simulink model is described in the works by S. Skogestad et al. [31], and is shown below as equation 5.1.

$$T_j = \sum_{i=1}^{NC} x_{j,i} T_{b,i} \qquad (5.1)$$

Equation 5.1 calculates a temperature estimate on each tray based on the liquid compositions present. The temperature of the mixture is estimated as the molar average of the boiling points of pure components in the liquid phase. Equation 5.1 will give a higher estimate than what is expected for ideal mixtures [31].

Method 2: Modified Boiling Point

The second method is a modification of the simple boiling point method and includes the vapour phase composition as shown below in equation 5.2 [31]:

$$T_j = \sum_{i=1}^{NC} \frac{x_{j,i} \cdot y_{j,i}}{2} \cdot T_{b,i} \qquad (5.2)$$

This method will usually provide a fairly accurate temperature estimate [31].

Method 3: Vapour Pressure Iteration

An alternative to the simple boiling point method is to use the vapour pressure equations to iterate on the temperature on every tray until Raoult's law as shown in equation 5.3 converges.

$$0 = P - \sum_{i=1}^{NC} x_i P_i^*(T) \qquad (5.3)$$

The iteration of equation 5.3 can be inserted into the regular Matlab script either directly or by using the command fsolve. However, because of the number of iterations required on every tray for every temperature for every value of the composition, the script runs very slowly so no results are achieved. The solution was to apply a differential algebraic equation (DAE) system with a mass matrix, which speeds up iterations significantly. However, at the moment there is no method available on how to solve DAE systems in Simulink, so the code had to be moved to pure m-files.

The introduction of equation 5.3 to the Matlab code merges a set of differential equations with an algebraic equation. This requires a DAE solver once the brute-force method is eliminated. A DAE solver is based on equation 5.4 below [32]:

$$M \frac{dy}{dt} = f(y, u) \qquad (5.4)$$

The parameter M represents the mass matrix, which indicates the presence of algebraic and differential equations by a 0 or a 1, respectively, usually diagonally. Equation 5.4 represents a general approach which allows for faster simulations [32].

The Matlab m-code with the DAE system approach is available in Appendix G, and the solver applied is ode15s, which is designed to handle stiff ODEs and DAEs.

5.2 Simulation Results - Temperature

The temperature profiles using the three different methods described in the previous section, as well as the literature results [1] are shown below in Figure 5.1 for the reactive distillation column. The temperatures are also summarized in Table 5.1 for easy comparison.

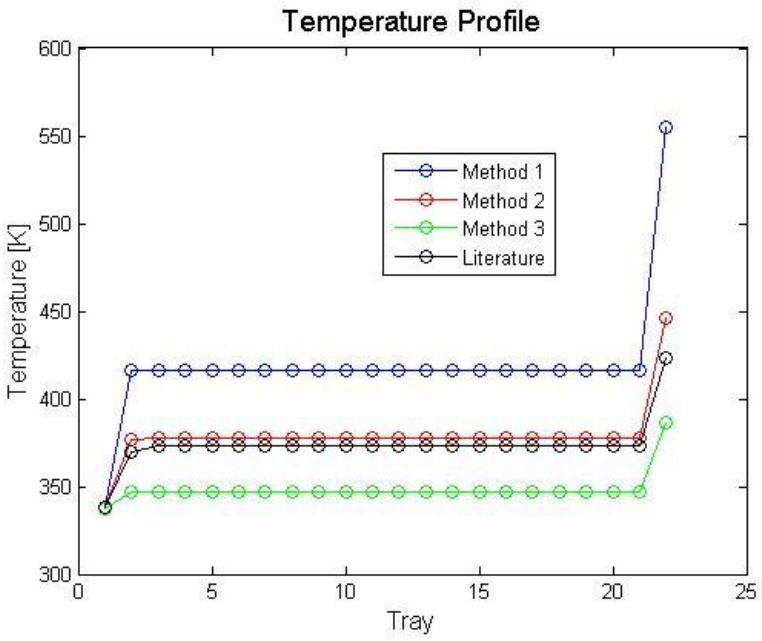

Figure 5.1: The temperature profile for the modified boiling point method

Table 5.1: The temperatures in the reactive column by methods 1-3

Column position	Method 1	Method 2	Method 3	Literature [1]
Condenser	337.9	337.9	337.7	338 ± 1
Tray 2	416.5	377.1	346.7	370 ± 1
Tray 3-21	416.6	377.2	346.7	373 ± 1
Reboiler	554.4	446.3	386.1	423 ± 1

Comments

The best estimation of the temperature is the modified boiling point method. However, the modified boiling point method has a significant error when calculating the reboiler temperature of approximately 23K. The reason for this error estimation is probably due to the fact that the product purity of the Simulink model was higher than for the model by Simasatitkul et al. However, this does not explain why the estimation is so spot-on for the remaining section of the column where there is too much methanol present compared to the Hysys model.

The reason for method 3 giving a lower temperature in the intermediate sections of the column is probably due to excess methanol present in this model compared to the literature, or errors in the vapour pressure equations. Method 1 gave the worst overall performance and overestimated the temperatures significantly. As mentioned in the theory section, this method usually reports a slightly higher temperature than displayed by ideal mixtures.

A quick evaluation of all the vapour pressure equations was performed by finding the vapour pressures at the respective boiling points for the compounds (which by definition should equal atmospheric pressure). However, the vapour pressure estimates of DG and MG at the boiling points showed relative errors of approximately 116% and 15% respectively from the atmospheric pressure. This means that the vapour pressure equations are clearly not a good fit for high temperature intervals, and probably not for the lower temperature intervals either. However, other estimation

methods are available. For now, the modified boiling point method will be applied as the temperature estimation method throughout the rest of this report. But if good alternative estimation methods are found for vapour pressure equations and perhaps even the activity coefficient is implemented, this could yield a good result.

6. Performance of the Model

This section provides an overview of the methods used to assess the performance of the model. The models performance is then compared to the results achieved by Simasatitkul et al. [1].

6.1 Conversion and Yield

The performance of a process is commonly measured in terms of yield and conversion. The conversion is a measure of how much of the limiting reagent is used up in the reaction, while the yield is a measure of how much product is obtained from the limiting reagent. The properties can be calculated by applying equations 6.1 and 6.2 below for the production of methyl linolein through transesterification reaction of methanol and trilinolein [1]:

$$Conversion = \frac{F_{0,Trilinolein} - F_{Trilinolein}}{F_{0,Trilinolein}} \quad (6.1)$$

$$Yield = \frac{F_{methyl\ linolein}}{3 \cdot F_{0,Trilinolein}} \quad (6.2)$$

6.2 Effect of Feed Temperature on Performance

To evaluate the performance of the model, the conversion and yield were calculated for varying feed temperatures, using the feed liquid fractions as given in Table 4.1. This is another way of comparing the dynamic Simulink model to the Hysys model of Simasatitkul et al, and the results are shown in Figure 6.1 and 6.2 below. The values for the yield and conversion for the model and the literature values at the initial feed temperature are given in Table 6.1 below.

Table 6.1: Conversion and yield at feed temperature

	Model	Literature
Conversion	99.68%	98.25% ± 0.05
Yield	98.48%	95.40% ± 0.05

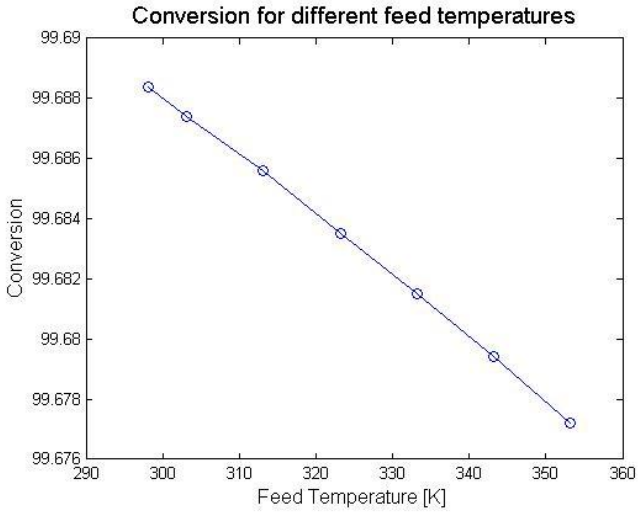

Figure 6.1: The change in conversion with regard to the feed temperature.

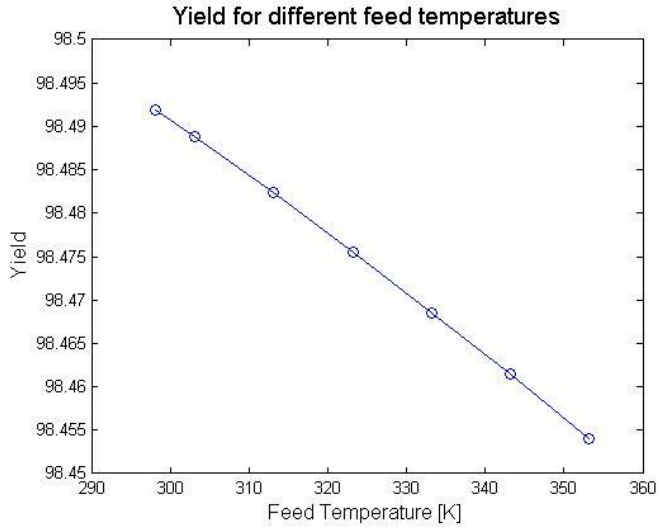

Figure 6.2: The change in yield with feed temperature

Both the yield and the conversion of the model are higher than the values reported by Simasatitkul et al, and vary less with the temperature. However, the trend displayed by the conversion and yield; an almost linear decrease with increasing temperature, is the same as for the model by Simasatitkul. The graphs by Simasatitkul et al. are shown below in Figures 6.3 and 6.4:

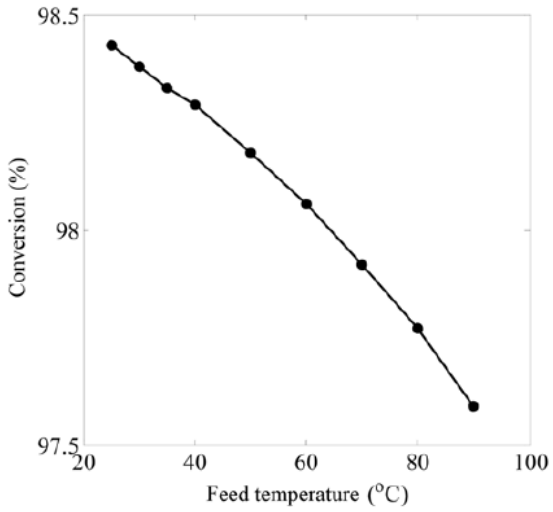

Figure 6.3: The effect of feed temperature on conversion [1].

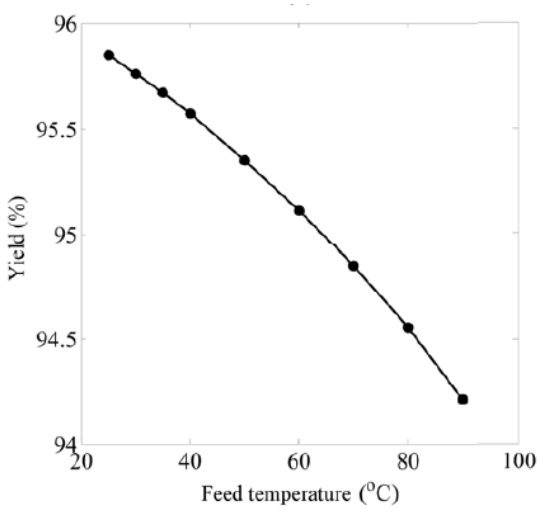

Figure 6.4: The effect of feed temperature on yield [1].

6.3 Number of Trays Necessary

This section will investigate the number of reactive trays required in the column and acompare the results to reported values [1].

Number of Reactive Trays

The number of reactive trays was plotted against the conversion and the yield in Figures 6.5 and 6.6 respectively.

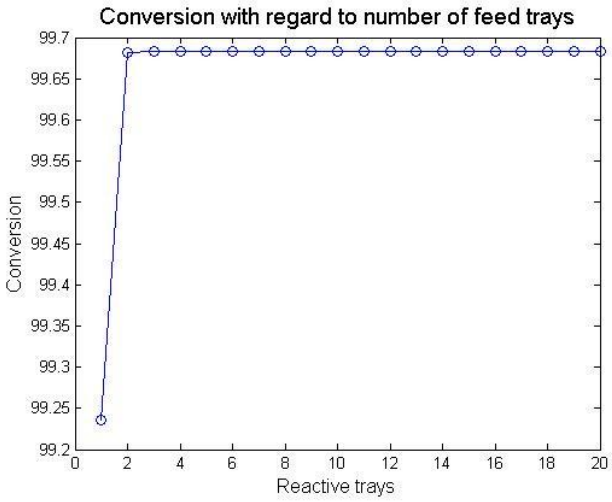

Figure 6.5: The conversion against the number of reactive trays in the column

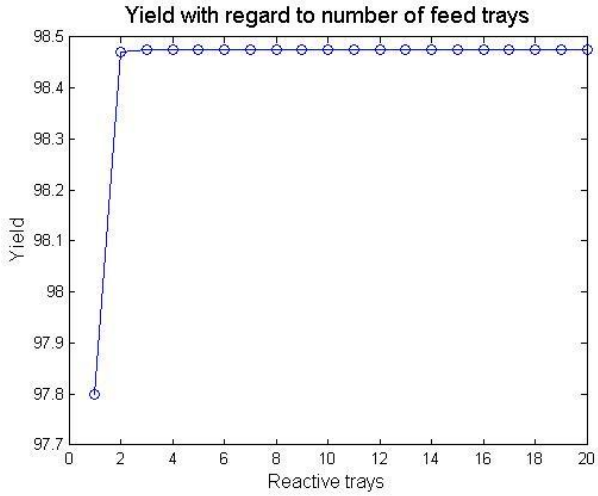

Figure 6.6: The yield plotted against the number of reactive trays.

From Figures 6.5 and 6.6 one can see that the conversion and yield will increase with an increasing number of trays, until it reaches a plateau after about 3 reactive trays. This is expected, and shows that the model follows the same trends as the published results by Simasatitkul et al. These results are given below in Figures 6.7 and 6.8. The conversions and yields recovered from the model are overall higher than in the literature, which is also the case here. The conversions and yields of the model also appear to vary slightly less with the number of reactive trays compared to the literature.

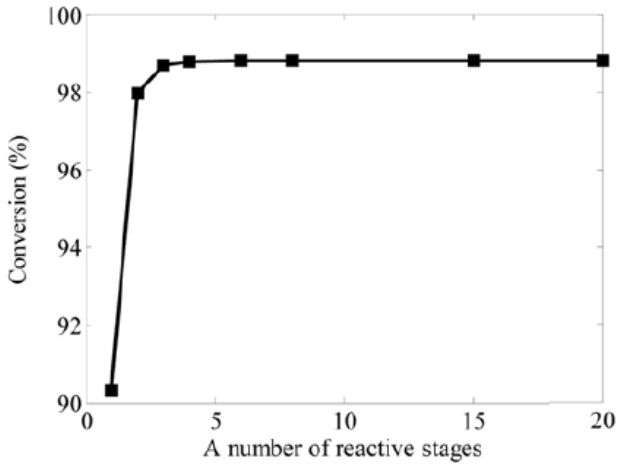

Figure 6.7: Literature plot of conversion against number of reactive stages [1].

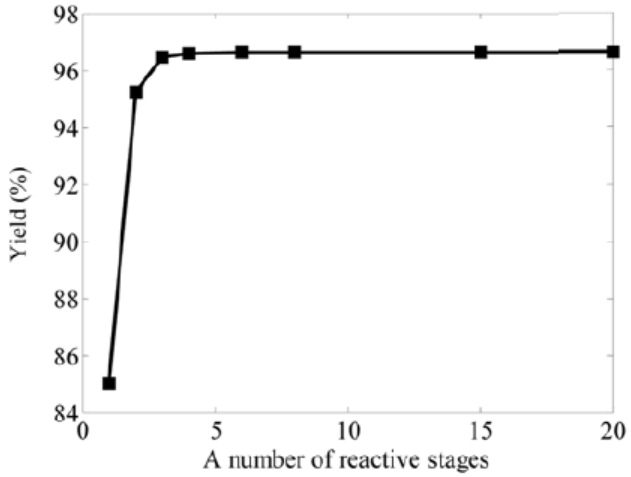

Figure 6.8: Literature plot of yield against number of reactive stages [1].

7. Summary and Discussion

This section will provide a more detailed overview and discussion of the challenges encountered while constructing the reactive distillation model. The aspects described here have been mentioned at earlier points in the report but are brought to attention again to summarize and highlight the most important qualities of the model. The discussion is divided into four parts: the column composition profile, liquid dynamics, temperature estimations and yield and conversion.

7.1 The Column Composition

The model was constructed in Simulink Matlab R2012a for the reactive distillation of linoleic esters from soybean oil to biodiesel. The model applied material steady-state balances for the distillation column with NC*NT states, with NT states represented the total molar holdups on each tray while the NC-1*NT states represented the individual molar holdups for five of the components. The reactive behaviour was approximated by introducing rate law equations and kinetic data from

Simasatitkul et al [1] for the linoleic esters. The change in concentration of the individual components due to reaction was converted to molar fractions and added to the material balances.

Modelling a reactive distillation column as a steady-state process is a debated process, and it has been suggested that mass transfer equations should be applied instead [2]. However, Alejski and Duprat [15] argue that the kinetics can be described by using the rate law and normal material balances. They introduced a plate efficiency to correct for the kinetic equilibrium not being reached on every stage.

Perhaps one of the most notable challenges with the model is the fact that the column profile of the mass fractions does not match the literature values. The intermediate sections of the column have too high values for methanol while the product contains too little methanol compared to the mass fractions reported by Simasatitkul et al. [1]. If the problem is due to the fact that chemical equilibrium is not reached, it may help to include plate efficiencies as described by Alejski and Duprat, or otherwise one may have to include mass transfer equations which would be a very extensive alteration.

It could also well be that the problem is related to the reaction kinetics, as the rate equations reported by Simasatitkul et al. differ from the equations derived from the rate law as applied to the dynamic model. The difference was first considered a misprint and consisted of the concentration of methanol being replaced by the concentration of biodiesel at two points; in the expression for change in concentration of DG and MG for the first and second reverse reaction respectively. When the error in the column profile was discovered, the same equations were implemented in the Simulink model. However, this gave a worse performance than the standard rate equations with higher amounts of methanol in the column and almost no glycerol present.

The relative volatility method compared to vapour phase estimations using Raoult's law gave very similar results throughout the column. Proper tuning of the relative volatility would allow for even better description of the systems behaviour and would also simplify the model. However, at the present this method did not perform well when the column was subject to disturbances. This may indicate that the relative volatilities would be better described by equations depending on temperature or composition.

The evaluation of the vapour pressure equations for DG and MG used in the Raoult's law method for estimating the compositions revealed a large error. These compounds are present in small amounts in the column, but because they have such low volatility, they may still influence temperature and vapour phase estimations. Several methods are available for estimation of critical parameters and vapour pressures, and these could be investigated further, as some of them may give better performance. If this would still yield a poor performance, the activity coefficient could be implemented through use of thermodynamic models such as UNIFAC/UNIQUAC.

Another problem with estimating the compositions in the model was the response of the model to a step change in the feed composition. The composition in the bottoms was very sensitive to changes in the feed fraction, and decreasing the feed ratio of methanol/trilinolein contributed to making the mass fraction of methanol in the bottoms negative. This is of course not possible and should be investigated further as it could be due to any number of the reasons already listed. However, the

result suggests that the column may become unstable (could lead to drift) when changes are introduced in the feed composition. This would require tight composition/temperature control.

7.2 Liquid Dynamics

The liquid dynamics were described using the Francis weir equation and assuming constant volume holdup and no foaming, while constant molar overflow and no vapour holdup was assumed for the vapour dynamics. The liquid feed fraction was calculated from the enthalpies of the feed at the dew point and bubble point. The assumption of no vapour holdup is reasonable as the pressure is quite low in the column. However, foaming will probably be present and thus the height over weir will actually be higher than the calculated value.

The weir height was estimated to be more than twice the height of a normal weir to provide extra residence time for the reaction. This may not be necessary as the reaction kinetics are quite fast. However, if plate efficiency was to be implemented as discussed by Alejski and Dupart, the required number of reactive trays would increase. The problem is then reduced to finding the least expensive option; decreasing the number of trays or increasing the height of the weirs.

In comparison with a normal distillation column, the dynamics of the reactive distillation column seemed reasonable. The holdups in the condenser and reboiler were reduced by a factor of 4 to save energy expenses, but they are still quite large compared to the nominal distillation column and can be reduced even further.

In response to disturbances in the feed flowrate and in the feed composition, the dynamics behaved as expected.

7.3 Temperature

The temperature was estimated using three different methods. Two methods used intermediate values of the boiling point and liquid/vapour fractions, while the third methods solved an algebraic iteration using the vapour pressures and Raoult's law. The third method had to be moved out of Simulink and into a regular m-code script to solve the DAE system using ode15s.

The best method for calculating the temperature overall was the modified boiling point method, (method 2). Method 2 calculated an average value for the boiling point on each tray by considering both the vapour phase and the liquid phase compositions, and had a relative error of approximately 23K for the reboiler and 5K for the column. The iterative Raoult's law method underestimated the column and the reboiler temperatures with a large deviation, while method 1 overestimated all the temperatures except the condenser.

The reason for the underestimations of Raoult's law could be due to the excess amounts of methanol present in the column of the model compared to the literature. This would decrease the overall boiling point of the mixture as methanol is the light key, and give lower temperature estimates. If a better estimation method for the composition in the column would be implemented, this problem might fix itself and Raoult's law might give the best estimation of the temperature.

7.4 Yield and Conversion

The yield and conversion achieved in the column for the model gave a better performance compared to the literature values. The yield and conversion both displayed the trends of the published work,

but varied less with the temperature and the number of reactive trays than expected. A probable reason for this behaviour is the lack of energy balances in the dynamic model, or the problems with the kinetic/chemical equilibrium implementations as discussed previously.

Many of the issues with the model are connected to how the Hysys model by Simasatitkul et al. was derived and on what grounds. If the Hysys model had been made available, it would be easier to establish why the differences occur, and maybe how to fix them. Several attempts have been made in order to contact the authors, but none have been successful.

8. Conclusion

The literature search in the beginning of the project coursework uncovered the article on reactive distillation from soybean oil by Simasatitkul et al. [1] from which much of the design and data of this project have been based. The modelling method applied is a simplified version of the work by Alejski and Duprat [15].

The reactive distillation model in Simulink Matlab was developed using the Francis' weir formula for liquid hydraulics, standard rate laws for the reaction kinetics and chemical equilibrium, molar balances for mass preservation and Raoult's law and relative volatilities for phase equilibrium behaviour. The temperature was estimated using a modified boiling point method and the performance of the model was evaluated by comparing it to published results [1] and by calculating the conversion and yields achieved.

The dynamic Simulink model produced represents the general behaviour of the reactive biodiesel process and shows the same trends as the literature data. However there are still some aspects that require further attention, as the model does not show identical behaviour to the simulation by Simasatitkul et al. The main deviation seems to be due to the implementation of the chemical equilibrium. This results in a higher content of methanol in the column. This error influences the rest of the parameters evaluated such as the temperature in the column, and the yield and conversion. The error could perhaps be improved by introducing plate efficiency as described by Alejski and Duprat [15] or by testing other methods for implementing the kinetics. The modification of the code should also contain a constraint on the molar flowrates so that it would not be possible to obtain negative flowrates. This occurred for the methanol flowrate in the bottoms when a disturbance in the feed composition was introduced.

9. Further Work

The obvious first step would be to ensure that the model behaves as expected. As mentioned earlier, there are still some challenges in this area concerning the compositions in the column, and unstable behaviour when disturbances occur in the feed composition. It is necessary to have a second look at the chemical equilibrium implementation, and a plate efficiency should be installed. If this does not fix the problem, one should consider implementing energy balances and/or using UNIFAC/UNIQUAC to correct for non-ideality in the phase equilibrium estimations.

The focus of the report was mainly on developing a simple model to describe the behaviour of a reactive distillation biodiesel plant. However, as a next step it would be interesting to look at optimising the column to achieve better performance. This could include for example finding the

optimal weir height, reboiler and condenser holdup, reboiler duty, reflux ratio and feed composition. Throughout this report it has been concluded that decreased feed temperature and no more than 3 reactive trays (assuming 100% efficiency) gave the best overall performance measured in terms of yield and conversion.

There is also a need for the development of a control structure for the reactive distillation column, as the model appears very sensitive to disturbances, especially disturbances in the feed composition. Temperature should be tightly controlled as it gives an indication of the composition. The reaction is also exothermic and may require cooling on the trays.

Finally, some more general aspects that require further work linked to biodiesel production through reactive distillation will be quickly mentioned. The first is that there is dire need for research on heterogeneous catalysts, as this would have great environmental benefits as well as further simplifying the process and reducing operational costs. Also, physical, thermodynamic and kinetic data are required in greater numbers and available with higher accuracy. This way, the model could be used for other sources of oils that put less of a strain on the environment and society, such as algae.

10. Nomenclature

Table 10.1: Abbreviations

AIChE	American Institute for Chemical Engineers
BD	Biodiesel, here also known as methyl linoleate
CAPEX	Capital costs
DAE	Differential algebraic equation
DG	Diglyceride, but usually refers to dilinolein
FAME	Fatty acid methyl ester
FFA	Free fatty acids
MetOH	Methanol
MG	Monoglyceride, but usually refers to monolinolein
MTBE	Methyl tert-butyl-ether
NC	Number of compounds
NT	Number of trays
RCM	Residue curve map
TAG	Triacylglycerol
TG	Trilinolein

Table 10.2: Greek symbols

α_c	Constant in the Riedel method
α_i	Relative volatility for component i.
γ_i	Liquid phase activity coefficent
ρ_L	Liquid density [kg/m^3]
ρ_l	Liquid density [kmol/m^3]
ρ_V	Vapour density [kg/m^3]
ψ_b	Constant in the Riedel method

Table 10.3: Symbols

A_i	Arrhenius constant for specific reaction [m^3/kmol h]
A_c	Total cross-sectional area of column [m^2]
B	Bottoms flowrate [kmol/h]
Cp_l	Liquid heat capacity [kJ/kmol K]
D	Distillate flowrate [kmol/h]
D_c	Column diameter [m]
E_a	Activation energy [kJ/mol]
F	Feed flowrate [kmol/h]
F_{LV}	Liquid-vapour flow factor
H_F	Enthalpy at feed [kJ/kmol]
ΔH_f	Standard heat of formation [kJ/kmol]
H_L	Enthalpy at bubble point [kJ/kmol]
h_{ow}	Height over weir [m]
HR	Molar holdup [kmol]
H_V	Enthalpy at dew point [kJ/kmol]
ΔH_{vap}	Standard heat of vaporisation [kJ/kmol]
h_w	Height of weir [m]
K_1	A constant in the flooding vapour velocity equation
k_i	Rate constant for reaction 1-6
L	Liquid flowrate [kmol/h]
L_{bf}	Liquid flowrate below feed [kmol/h]
L_{of}	Liquid flowrate over feed [kmol/h]
L_w	Liquid mass flowrate [kg/s]
l_w	Length of weir [m]
M	Mass matrix
M_i	The molar change of component i due to reaction [kmol]
M_w	Molecular weight [kg/kmol]
N_A	Number of atoms
P	Pressure [atm]
P_c	Critical pressure [atm]
P_i^*	Vapour pressure of compound i [atm]
P_r	Reduced pressure
q	Fraction of feed that is saturated liquid
R	Gas constant [J/K mol]
Ref	The reflux [kmol/h]
T	Temperature [K]
T_b	Boiling temperature [K]
T_c	Critical temperature [K]
T_r	Reduced temperature
u_f	Flooding vapour velocity, [m/s]
Vb	Vapour boilup [kmol/h]
V_{bf}	Vapour flowrate below feed [kmol/h]
V_{of}	Vapour flowrate over feed [kmol/h]
VR	Volume holdup [m^3]
V_w	Vapour mass flowrate [kg/s]
x_i	Liquid molar fraction of component i
$x_{w,i}$	Liquid mass fraction of component i
y_i	Vapour molar fraction of component i

11. Bibliography

1. Simasatitkul, L., et al., *Reactive distillation for biodiesel production from soybean oil.* Korean Journal of Chemical Engineering, 2011. **28**(3): p. 649-655.
2. Towler, G.P. and S.J. Frey, *Reactive Distillation*, in *Reactive Separation Process*, S. Kulprathipanja, Editor. 2002, Taylor & Francis. p. 18-48.
3. *Annual Energy Outlook 2012 - with Projections to 2035*. June 2012; Available from: www.eia.gov/forecasts/aeo.
4. *BP Statistical Review of World Energy June 2012*. Available from: http://goo.gl/5wTL9.
5. Drapcho, C.M., N.P. Nhuan, and T.H. Walker, *Biofuels Engineering Process Technology*. 2008: McGraw-Hill.
6. Kiss, A.A. and C.S. Bildea, *A review of biodiesel production by integrated reactive separation technologies.* Journal of Chemical Technology & Biotechnology, 2012. **87**(7): p. 861-879.
7. Sundmacher, K. and A. Kienle, *Reactive Distillation - Status and Future Directions*. 2003: Wiley-VCH.
8. Hammond, E.G., et al., *Soybean Oil*, in *Bailey's Industrial Oil and Fat Products*, F. Shahidi, Editor. 2005. p. 577-604.
9. *DIPPR 801 Database*. Available from: http://dippr.byu.edu/students/.
10. Costenoble, O., et al. *Improvements needed for the biodiesel standard EN 14214*. 2008.
11. *Biodiesel Standards*. [cited 2012 09/11]; Available from: http://www.biofuelsystems.com/specification.htm.
12. Knothe, G., J. Krahl, and J.V. Gerpen, *The Biodiesel Handbook*. 2 ed. 2010: AOCS Press.
13. Malone, M.F. and M.F. Doherty, *Reactive Distillation.* Industrial & Engineering Chemistry Research, 2000. **39**(11): p. 3953-3957.
14. Leet, W.A. and S. Kulprathipanja, *Reactive Separation Processes*, in *Reactive Separation Process*, S. Kulprathipanja, Editor. 2002, Taylor & Francis. p. 1-16.
15. Alejski, K. and F. Duprat, *Dynamic simulation of the multicomponent reactive distillation.* Chemical Engineering Science, 1996. **51**(18): p. 4237-4252.
16. Leung, D.Y.C., X. Wu, and M.K.H. Leung, *A review on biodiesel production using catalyzed transesterification.* Applied Energy, 2010. **87**(4): p. 1083-1095.
17. Skouras, S. *MulticomA - nonlinear model of a continuous distillation column with multicomponent mixture*. 2001; Available from: http://goo.gl/OF7qu.
18. Jhon, Y.H. and T.-h. Lee, *Dynamic simulation for reactive distillation with ETBE synthesis.* Separation and Purification Technology, 2003. **31**(3): p. 301-317.
19. Rahul, M., et al., *An efficient algorithm for rigorous dynamic simulation of reactive distillation columns.* Computers & Chemical Engineering, 2009. **33**(8): p. 1336-1343.
20. *1-Monolinoleoyl-rac-glycerol*. Available from: http://goo.gl/Ku39P.
21. *1,2-dilinoleoylglycerol*. Available from: http://goo.gl/45b0m.
22. Reid, R.C., J.M. Prausnitz, and B.E. Poling, *The Properties of Gases & Liquids*. 4 ed. 1987: McGraw-Hill.
23. Issariyakul, T. and A.K. Dalai, *Comparative kinetics of transesterification for biodiesel production from palm oil and mustard oil.* The Canadian Journal of Chemical Engineering, 2012. **90**(2): p. 342-350.
24. Geankoplis, C.J., *Vapor-Liquid Separation Processes*, in *Transport Processes and Separation Process Principles*. 2003, Prentice Hall. p. 696-759.
25. Buckley, P.S., W.L. Luyben, and J.P. Shunta, *Design of Distillation Control Systems*. 1985: Edward Arnold.
26. Fredenslund, A., J. Gmehling, and P. Rasmussen, *vapor-liquid equilibria using UNIFAC*. 1977: Elsevier Scientific Publishing Company.

27. Sinnott, R.K., *Coulson and Richardson's Chemical Engineering Volume 6 - Chemical Engineering Design (4th Edition)*, Elsevier.
28. *Vapor-Liquid Equilibria (VLE) - Background*. Available from: http://www.et.byu.edu/~rowley/VLEfinal/background.htm.
29. Helbæk, M. and S. Kjelstrup, *Fysikalsk kjemi*. 2 ed. 1999: Fagbokforlaget.
30. Skogestad, S., *The Dos and Don'ts of Distillation Column Control.* Chemical Engineering Research and Design, 2007. **85**(1): p. 13-23.
31. Halvorsen, I.J. and S. Skogestad, *Distillation Theory*, in *Encyclopedia of Separation Science*, I.D. Wilson, Editor. 2000, Academic Press. p. 1117-11134.
32. Skogestad, S., *Chemical and Energy Process Engineering*. 2008: CRC Press Taylor & Francis Group.
33. *1-Monolinolein(2277-28-3)*. Available from: http://goo.gl/zu4r9.
34. *1,3-Dilinolein(15818-46-9)*. Available from: http://goo.gl/UugMF.
35. Velasco, S., et al., *A predictive vapor-pressure equation.* The Journal of Chemical Thermodynamics, 2008. **40**(5): p. 789-797.

A. Matlab Scripts

This appendix gives a print of the Matlab files that constitute the dynamic model. The Matlab files are closely correlated with the Simulink model, and cannot run without it. A print of the Simulink model is given in the next appendix. Dynamic versions of all files have been provided electronically.

A.2 The main file

The main script is given below, and mainly contains specifications for the simulation.

```
%Basic model for reactive distillation column for biodiesel production
%By Emilie Øritsland Houge
%clc, clear all, close all
format long

%% Feed flows
%     metOH/TG/DG/MG/GL/BD
F = [300 50 0 0 0 0];      % Feed flowrates [kmol/h]
F_new = [286.36 63.64 0 0 0 0];  % Disturbance in feed [kmol/h]
F0 = sum(F);               % Total feed flowrate[kmol/h]
x_in = F/F0;               % Molar fractions
x_new = F_new/F0;          % Disturbance molar fractions [kmol/h]
Mw = [32.0 879.3844 616.95 354.52 92.094 294.47]'; %Molecular weights [kg/kmol]

%% Distillation data
Ntrays = 20;         %Number of trays
Ntrays_react = 3;    %Number of reactive trays
NC = 6;              %Number of compounds
D = 140.05;          %Distillate [kmol/h]
Vb = 430;            %Vapour boil up [kmol/h]
B = 209.95;          %Bottoms, [kmol/h]
Ref = 3;             %Reflux ratio
Con_set = 25;        %Holdup condenser [kmol]
Reb_set = 25;        %Holdup reboiler [kmol]


%% Simulation
t0 = 0;     %[h]
tfin = 20;  %[h]

tic
sim('reactivedistillation_sfcn2')
toc
```

A.3 The s-function

The s-function is a longer code which contains all equations and iterations necessary to simulate the process.

```
function Distillation_sfcn2(block)
% This is a level 2 sfcn in simulink describing the production of biodiesel
% through reactive distillation
% The compounds are always listed in the following order: metOH/TG/DG/MG/GL/BD


%% Establishing the number of inputs and outputs:
nu = 6;
ny = 7;
Ntrays = 20;
NC = 6;

% block definitions
block.NumInputPorts  = nu;
block.NumOutputPorts = ny;
```

```
% Setup port properties to be inherited or dynamic
block.SetPreCompInpPortInfoToDynamic;
block.SetPreCompOutPortInfoToDynamic;

for i = 1:nu
    block.InputPort(i).Dimensions = 1;
    block.InputPort(i).DirectFeedthrough = true;
end
block.InputPort(2).Dimensions = NC; %The second input port is the feed molar
fraction


for i = 1:ny
    block.OutputPort(i).Dimensions = 1;
end

block.OutputPort(1).Dimensions = NC;
block.OutputPort(2).Dimensions = NC;
block.OutputPort(3).Dimensions = (Ntrays+2)*(NC-1);
block.OutputPort(4).Dimensions = Ntrays+2;
block.OutputPort(5).Dimensions = Ntrays+2;
block.OutputPort(6).Dimensions = Ntrays+1;
block.OutputPort(7).Dimensions = Ntrays+1;

block.SampleTimes = [0 0];

% Setup Dwork
block.NumContStates = (Ntrays+2)*(NC-1)+Ntrays+2;

block.RegBlockMethod('InitializeConditions',    @InitializeConditions);
block.RegBlockMethod('Outputs',                 @Outputs);
block.RegBlockMethod('Derivatives',             @Derivatives);
block.RegBlockMethod('SetInputPortSamplingMode',@SetInpPortFrameData);


function SetInpPortFrameData(block, idx, fd)

block.InputPort(idx).SamplingMode = fd;
for i = 1:block.NumOutputPorts
    block.OutputPort(i).SamplingMode = fd;
end


function InitializeConditions(block)

load steadystate % x0
block.ContStates.Data = steadystate;

function Outputs(block)

% Important Parameters
Ntrays = 20;                        %Number of trays in column
NC = 6;                             %Number of compounds
Mw = [32.0 879.3844 616.95 354.52 92.094 294.47]; %Molecular weights [kg/kmol]
Ntrays_react = 3;                   %Number of reactive trays
alpha = [1 0.01 0.01 0.02 0.05 0.03];             %Relative volatilities
Dc = 1.8564;                        %Diameter of column [m]
lw = 1.4295;                        %Length of weir [m]
hw = 0.20;                          %Heigth of weir [m]
Tb = [337.85 895.3 942.6 758.2 561.0 619.15];     %Boiling points [K]
q = 1.028;                          %Fraction of liquid in feed

%% Key Variables
% State variables
x = block.ContStates.Data(1:(Ntrays+2)*(NC-1)); %Molar fractions
H = block.ContStates.Data(((Ntrays+2)*(NC-1)+1):NC*(Ntrays+2)); %Molar holdup
xL = reshape(x,Ntrays+2,5);  %Reshaping into a matrix
```

```
HL = reshape(H,Ntrays+2,1);  %Reshaping into a vector
%We still use the sequence: MetOH/TG/DG/MG/GL/BD

% Disturbances
F0   = block.InputPort(1).Data;
x_in  = block.InputPort(2).Data;

% Manipulation
D   = block.InputPort(3).Data;
Vb   = block.InputPort(4).Data;
Ref   = block.InputPort(5).Data;
B   = block.InputPort(6).Data;

%% Calculation of compositions and temperature by method 1

T = 373.15*ones(Ntrays+2,1); %Setting the initial temperature
XX = zeros(Ntrays+2,NC);  x_BD = zeros(Ntrays+2,1);
y = zeros(Ntrays+2,NC-1); y_BD = zeros(Ntrays+2,1);

for i = 1:Ntrays+2
    %Molar fraction of BD:
    x_BD(i,1) = 1 - sum(xL(i,:));
    XX(i,:) = [xL(i,:) x_BD(i,1)];

    %Temperature by Method 1:
%    T(i,1) = sum(Tb.*XX(i,:));  %The temperature on each tray is the sum of the
individual boiling points

    %Vapour composition by relative volatilities:
%      yy = (alpha.*XX(i,:))/sum(alpha.*XX(i,:));
%      y(i,1) = yy(1,1); y(i,2) = yy(1,2); y(i,3) = yy(1,3); y(i,4) = yy(1,4);
y(i,5) = yy(1,5);
% %
% %     %Temperature by Method 2:
%      T(i,1) = sum(((XX(i,:) + yy)/2).*Tb);
end

%% Calculations of densities in the liquid phase:

% Initialising sizes
rho_MetOH = ones(Ntrays+2,1); rho_TG = ones(Ntrays+2,1); rho_GL = ones(Ntrays+2,1);
rho_BD = ones(Ntrays+2,1); rho_DG = ones(Ntrays+2,1); rho_MG = ones(Ntrays+2,1);
rho = [rho_MetOH rho_TG rho_DG rho_MG rho_GL rho_BD];
rho_l = ones(Ntrays+2,1); rho_L = ones(Ntrays+2,1); x_wt = zeros(Ntrays+2,NC);

%The constants
Ar_met = 2.3267; Br_met = 0.27073; Cr_met = 512.5; Dr_met = 0.24713;
Ar_TG = 0.026085; Br_TG = 0.14259; Cr_TG = 934.6; Dr_TG = 0.28571;
Ar_GL = 0.92382; Br_GL = 0.24386; Cr_GL = 850; Dr_GL = 0.22114;
Ar_BD = 0.20469; Br_BD = 0.23737; Cr_BD = 767.4; Dr_BD = 0.28571;

for i = 1:Ntrays+2
      rho_MetOH(i,1) = Ar_met/(Br_met^(1+(1-(T(i,1)/Cr_met))^Dr_met));
      rho_TG(i,1) = Ar_TG/(Br_TG^(1+(1-(T(i,1)/Cr_TG))^Dr_TG));
      rho_GL(i,1) = Ar_GL/(Br_GL^(1+(1-(T(i,1)/Cr_GL))^Dr_GL));
      rho_BD(i,1) = Ar_BD/(Br_BD^(1+(1-(T(i,1)/Cr_BD))^Dr_BD));
      rho_DG(i,1) = ((2/3)*rho_TG(i,1)) + ((1/3)*rho_BD(i,1)); %We assume that the
density of DG and MG can be
      rho_MG(i,1) = ((1/3)*rho_TG(i,1)) + ((2/3)*rho_BD(i,1)); %approximated by the
densities of BD and TG
      rho(i,:) = [rho_MetOH(i,1) rho_TG(i,1) rho_DG(i,1) rho_MG(i,1) rho_GL(i,1)
rho_BD(i,1)];
      rho_l(i,1) = sum(rho(i,:).*XX(i,:));          %A common liquid density for
the tray [kmol/m3]
      x_wt(i,:) = (XX(i,:)*HL(i,1).*Mw)/sum(XX(i,:)*HL(i,1).*Mw); %Weight fraction
      rho_L(i,1) = sum(rho(i,:).*Mw.*x_wt(i,:));    %A common liquid density for
the tray [kg/m3]
end
```

```
%% Calculating the flowrates in the column
% Initializing sizes
V = ones(Ntrays+1,1);  %V is a vector of the molar vapor flows in the column
L = ones(Ntrays+1,1);  %L is a vector of the different trays in the column.

% Applying Francis weir for the liquid flowrates
how = ones(Ntrays,1); Lw = ones(Ntrays,1);
for i = 1:Ntrays
      how(i,1) = (HL(i+1,1)-(pi*hw*rho_l(i+1,1)*0.88*(Dc/2)^2))/(pi*0.88*(Dc/2)^2);
%Calculation of how
      if how(i,1) <0
          Lw(i+1,1) = 0;
          L(i+1,1) = 0;
      else
          Lw(i+1,1) = ((how(i,1)*10^3)/750)^1.5*rho_L(i+1,1)*lw;    %Francis weir
[kg/s]
          L(i+1,1) = (Lw(i+1,1)*3600)/sum(XX(i+1,:).*Mw);           %Liquid flow
[kmol/h]
      end
end

% Vapour flowrates
V(Ntrays+1,1) = Vb;

% Assuming constant molar overflow for vapour flowrates
for i = 2:Ntrays
    V(i,1) = V(Ntrays+1,1);
end

% Correction for the feed:
V(1,1) = V(2,1) + ((1-q)*F0);

% Molar balances over the top and the bottom:
L(1,1) = Ref;

%% Calculating the vapour compositions by vapour pressures, and temperature by
method 2
P = ones(Ntrays+2,1);
%Parameters necessary to calculate vapour pressures:
    A_met = 82.718; B_met = -6.9045*10^3; C_met = -8.8622; D_met = 7.4664*10^-6;
E_met = 2;
    A_TG = 234.71; B_TG = -3.4699*10^4; C_TG = -27.25; D_TG = 1.5475*10^-18; E_TG =
6;
    A_DG = -15.931; B_DG = -2111.0; C_DG = 2.4303; D_DG = 8.0567*10^-21; E_DG = 6;
    A_MG = 118.95; B_MG = -2.0181*10^4; C_MG = -14.32; D_MG = 9.148*10^-19; E_MG =
6;
    A_GL = 99.986; B_GL = -1.3808*10^4; C_GL = -10.088; D_GL = 3.5712*10^-19; E_GL
= 6;
    A_BD = 105.47; B_BD = -1.4531*10^4; C_BD = -10.986; D_BD = 2.5735*10^-18; E_BD
= 6;

for j = 1:Ntrays+2
    %Vapour pressure equations
    P_met = 9.869*(10^-6)*exp(A_met + (B_met/T(j,1)) + (C_met*log(T(j,1))) +
(D_met*T(j,1)^E_met));
    P_TG = 9.869*(10^-6)*exp(A_TG + (B_TG/T(j,1)) + (C_TG*log(T(j,1))) +
(D_TG*T(j,1)^E_TG));
    P_DG = 9.869*exp(A_DG + (B_DG/T(j,1)) + (C_DG*log(T(j,1))) +
(D_DG*T(j,1)^E_DG));
    P_MG = 9.869*exp(A_MG + (B_MG/T(j,1)) + (C_MG*log(T(j,1))) +
(D_MG*T(j,1)^E_MG));
    P_GL = 9.869*(10^-6)*exp(A_GL + (B_GL/T(j,1)) + (C_GL*log(T(j,1))) +
(D_GL*T(j,1)^E_GL));
    P_BD = 9.869*(10^-6)*exp(A_BD + (B_BD/T(j,1)) + (C_BD*log(T(j,1))) +
(D_BD*T(j,1)^E_BD));
    %Raoults law
```

```
    P(j,1) = P_met*xL(i,1) + P_TG*xL(i,2) + P_DG*xL(i,3) + P_MG*xL(i,4) +
P_GL*xL(i,5) + P_BD*x_BD(i,1);
    y(j,1) = (P_met*xL(i,1))/P(j,1);
    y(j,2) = (P_TG*xL(i,2))/P(j,1);
    y(j,3) = (P_DG*xL(i,3))/P(j,1);
    y(j,4) = (P_MG*xL(i,4))/P(j,1);
    y(j,5) = (P_GL*xL(i,5))/P(j,1);
    y_BD(j,1) = 1- sum(y(j,:));
    yy = [y(j,:) y_BD(j,1)];

%     % Temperature by method 2:
    T(j,1) = sum(((XX(j,:) + yy)/2).*Tb);
end




%% Determining distillate and bottoms flow
%Determination of the distillate flow
vD = D*XX(1,:);       % partial molar flows (kmol/h)

%Determination of the bottoms flow
vB = B*XX(Ntrays+2,:); % partial molar flows (kmol/h)


%% Output variables
block.OutputPort(1).Data = vD;
block.OutputPort(2).Data = vB;
block.OutputPort(3).Data = x;
block.OutputPort(4).Data = H;
block.OutputPort(5).Data = T;
block.OutputPort(6).Data = L;
block.OutputPort(7).Data = V;


function Derivatives(block)
%% Important parameters
Ntrays = 20;                %Number of trays
NC = 6;                     %Number of compounds
R = 8.314472*10^(-3);       %Gas constant [kJ/K*mol]
Mw = [32.0 879.3844 616.95 354.52 92.094 294.47]; %Molecular weights [kg/kmol]
Ntrays_react = 3;           %Number of reactive trays
Tb = [337.85 895.3 942.6 758.2 561.0 619.15];
q = 1.028;                  %Liquid feed fraction
Dc = 1.8564;                %Diameter of column [m]
lw = 1.4295;                %Length of weir [m]
hw = 0.20;                  %Heigth of weir [m]
alpha = [1 0.01 0.01 0.02 0.05 0.03];   %Relative volatilities

%% Variables
% State variables
  x = block.ContStates.Data(1:(Ntrays+2)*(NC-1));
  H = block.ContStates.Data(((Ntrays+2)*(NC-1)+1):NC*(Ntrays+2));
  xL = reshape(x,Ntrays+2,NC-1);
  HL = reshape(H,Ntrays+2,1);

% Disturbances
  F0   = block.InputPort(1).Data;
  x_in = block.InputPort(2).Data;
%The input F0 is the flowrate [kmol/h] and x_in is the composition.
%The composition is given in the following order: MetOH/TG/DG/MG/GL/BD

% Manipulation
  D   = block.InputPort(3).Data;
  Vb = block.InputPort(4).Data;
  Ref = block.InputPort(5).Data;
  B = block.InputPort(6).Data;
```

```
%% Calculation of temperatures and compositions

%Calculating the temperature on each tray:
T = 373.15*ones(Ntrays+2,1); %Setting the initial temperature
XX = zeros(Ntrays+2,NC);  x_BD = zeros(Ntrays+2,1);
y = zeros(Ntrays+2,NC-1); y_BD = zeros(Ntrays+2,1);

for i = 1:Ntrays+2
    x_BD(i,1) = 1 - sum(xL(i,:));
    XX(i,:) = [xL(i,:) x_BD(i,1)];

%     %Temperature by method 1:
%    T(i,1) = sum(Tb.*XX(i,:));
%     %Vapour phase composition by relative volatilities:
%     yy = (alpha.*XX(i,:))/sum(alpha.*XX(i,:));
%     y(i,1) = yy(1,1); y(i,2) = yy(1,2); y(i,3) = yy(1,3); y(i,4) = yy(1,4);
y(i,5) = yy(1,5);
%     %Temperature by method 2:
%     T(i,1) = sum(((XX(i,:) + yy)/2).*Tb);
end

%% Calculations of densities in the liquid phase:

% Initialising sizes
rho_MetOH = ones(Ntrays+2,1); rho_TG = ones(Ntrays+2,1); rho_GL = ones(Ntrays+2,1);
rho_BD = ones(Ntrays+2,1); rho_DG = ones(Ntrays+2,1); rho_MG = ones(Ntrays+2,1);
rho = [rho_MetOH rho_TG rho_DG rho_MG rho_GL rho_BD];
rho_l = ones(Ntrays+2,1); rho_L = ones(Ntrays+2,1); x_wt = zeros(Ntrays+2,NC);

% The constants
Ar_met = 2.3267; Br_met = 0.27073; Cr_met = 512.5; Dr_met = 0.24713;
Ar_TG = 0.026085; Br_TG = 0.14259; Cr_TG = 934.6; Dr_TG = 0.28571;
Ar_GL = 0.92382; Br_GL = 0.24386; Cr_GL = 850; Dr_GL = 0.22114;
Ar_BD = 0.20469; Br_BD = 0.23737; Cr_BD = 767.4; Dr_BD = 0.28571;

for i = 1:Ntrays+2
    %Densities [kmol/m3]
      rho_MetOH(i,1) = Ar_met/(Br_met^(1+(1-(T(i,1)/Cr_met))^Dr_met));
      rho_TG(i,1) = Ar_TG/(Br_TG^(1+(1-(T(i,1)/Cr_TG))^Dr_TG));
      rho_GL(i,1) = Ar_GL/(Br_GL^(1+(1-(T(i,1)/Cr_GL))^Dr_GL));
      rho_BD(i,1) = Ar_BD/(Br_BD^(1+(1-(T(i,1)/Cr_BD))^Dr_BD));
      rho_DG(i,1) = ((2/3)*rho_TG(i,1)) + ((1/3)*rho_BD(i,1));
      rho_MG(i,1) = ((1/3)*rho_TG(i,1)) + ((2/3)*rho_BD(i,1));
      rho(i,:) = [rho_MetOH(i,1) rho_TG(i,1) rho_DG(i,1) rho_MG(i,1) rho_GL(i,1)
rho_BD(i,1)];
      %A common liquid density for the tray [kmol/m3]:
      rho_l(i,1) = sum(rho(i,:).*XX(i,:));
      %Weight fractions:
      x_wt(i,:) = (XX(i,:)*HL(i,1).*Mw)/sum(XX(i,:)*HL(i,1).*Mw);
      %A common liquid density for the tray [kg/m3]
      rho_L(i,1) = sum(rho(i,:).*Mw.*x_wt(i,:));
end

%% Calculating the flowrates in the column
% Initializing sizes
V = ones(Ntrays+1,1);  %V is a vector of the molar vapor flows in the column
L = ones(Ntrays+1,1);  %L is a vector of the different trays in the column.

% Applying Francis weir for the liquid flowrates
how = ones(Ntrays,1); Lw = ones(Ntrays,1);
for i = 1:Ntrays
    %Calculation of height over weir [m]:
      how(i,1) = (HL(i+1,1)-(pi*hw*rho_l(i+1,1)*0.88*(Dc/2)^2))/(pi*0.88*(Dc/2)^2);
      if how(i,1) <0
          %Ensures no negative flowrates within column
          Lw(i+1,1) = 0;
          L(i+1,1) = 0;
      else
```

```
            %Francis weir [kg/s]
            Lw(i+1,1) = ((how(i,1)*10^3)/750)^1.5*rho_L(i+1,1)*lw;
            %Liquid flowrate [kmol/h]
            L(i+1,1) = (Lw(i+1,1)*3600)/sum(XX(i+1,:).*Mw);
        end
end

% Vapour flowrates
V(Ntrays+1,1) = Vb;

%Assume constant molar flowrate:
for i = 2:Ntrays
    V(i,1) = V(Ntrays+1,1);
end

% Correction for the feed:
V(1,1) = V(2,1) + ((1-q)*F0);

% Molar balances over the top:
L(1,1) = Ref;   %The first liquid molar flow is equal to the reflux.


%% Calculating the vapour compositions by vapour pressures + temperature by method
2
 %Parameters necessary to calculate vapour pressures:
A_met = 82.718; B_met = -6.9045*10^3; C_met = -8.8622; D_met = 7.4664*10^-6; E_met
= 2;
A_TG = 234.71; B_TG = -3.4699*10^4; C_TG = -27.25; D_TG = 1.5475*10^-18; E_TG = 6;
A_DG = -15.931; B_DG = -2111.0; C_DG = 2.4303; D_DG = 8.0567*10^-21; E_DG = 6;
A_MG = 118.95; B_MG = -2.0181*10^4; C_MG = -14.32; D_MG = 9.148*10^-19; E_MG = 6;
A_GL = 99.986; B_GL = -1.3808*10^4; C_GL = -10.088; D_GL = 3.5712*10^-19; E_GL = 6;
A_BD = 105.47; B_BD = -1.4531*10^4; C_BD = -10.986; D_BD = 2.5735*10^-18; E_BD = 6;
P = ones(Ntrays+2,NC);

for j = 1:Ntrays+2
    %Vapour pressure equations
    P_met = 9.869*(10^-6)*exp(A_met + (B_met/T(j,1)) + (C_met*log(T(j,1))) +
(D_met*T(j,1)^E_met));
    P_TG = 9.869*(10^-6)*exp(A_TG + (B_TG/T(j,1)) + (C_TG*log(T(j,1))) +
(D_TG*T(j,1)^E_TG));
    P_DG = 9.869*exp(A_DG + (B_DG/T(j,1)) + (C_DG*log(T(j,1))) +
(D_DG*T(j,1)^E_DG));
    P_MG = 9.869*exp(A_MG + (B_MG/T(j,1)) + (C_MG*log(T(j,1))) +
(D_MG*T(j,1)^E_MG));
    P_GL = 9.869*(10^-6)*exp(A_GL + (B_GL/T(j,1)) + (C_GL*log(T(j,1))) +
(D_GL*T(j,1)^E_GL));
    P_BD = 9.869*(10^-6)*exp(A_BD + (B_BD/T(j,1)) + (C_BD*log(T(j,1))) +
(D_BD*T(j,1)^E_BD));
    %Raoults law:
    P(j,1) = P_met*xL(i,1) + P_TG*xL(i,2) + P_DG*xL(i,3) + P_MG*xL(i,4) +
P_GL*xL(i,5) + P_BD*x_BD(i,1);
    y(j,1) = (P_met*xL(i,1))/P(j,1);
    y(j,2) = (P_TG*xL(i,2))/P(j,1);
    y(j,3) = (P_DG*xL(i,3))/P(j,1);
    y(j,4) = (P_MG*xL(i,4))/P(j,1);
    y(j,5) = (P_GL*xL(i,5))/P(j,1);
    y_BD(j,1) = 1- sum(y(j,:));
    yy = [y(j,:) y_BD(j,1)];
    %Temperature by method 2:
    T(j,1) = sum(((XX(j,:) + yy)/2).*Tb);
end

%% Calculation of the kinetics in the liquid phase:

%The sizes of the kinetic constants:
k1 = ones(Ntrays+2,1); k2 = ones(Ntrays+2,1); k3 = ones(Ntrays+2,1);
k4 = ones(Ntrays+2,1); k5 = ones(Ntrays+2,1); k6 = ones(Ntrays+2,1);
```

```
for i = 1:Ntrays+2
%Kinetic data for the reaction
k1(i) = 3.9*3600*(10^7)*exp(-54.9987/(R*T(i,1)));    %rate constants [m3/kmol*h]
k2(i) = 5.78*3600*(10^5)*exp(-41.5555/(R*T(i,1)));
k3(i) = 5.906*3600*(10^12)*exp(-83.0942/(R*T(i,1)));
k4(i) = 9.888*3600*(10^9)*exp(-61.2496/(R*T(i,1)));
k5(i) = 5.335*3600*(10^3)*exp(-26.8655/(R*T(i,1)));
k6(i) = 2.1*3600*(10^4)*exp(-40.1162/(R*T(i,1)));
end

%We need to convert the molar input to concentrations in order to calculate
%the reaction outputs:
C = zeros(Ntrays_react,6);
R = zeros(Ntrays_react,6);
M = zeros(size(C));
Msum = zeros(Ntrays_react,1);
for i = 1:Ntrays_react
   vH = HL(i+1,1)*XX(i+1,:);        %Molar holdup per component
   vr = sum(vH./rho(i+1,:));        %volume holdup
   C(i,:) = vH/vr;                  %concentration of each component
%The reactions. R is the gain/loss in [kmol/h]
R_TG = -(k1(i+1)*C(i,2)*C(i,1)) + (k2(i+1)*C(i,3)*C(i,6));
R_DG = (k1(i+1)*C(i,2)*C(i,1)) - (k2(i+1)*C(i,3)*C(i,6)) - (k3(i+1)*C(i,3)*C(i,1))
+ (k4(i+1)*C(i,4)*C(i,6));
R_MG = (k3(i+1)*C(i,3)*C(i,1)) - (k4(i+1)*C(i,4)*C(i,6)) - (k5(i+1)*C(i,4)*C(i,1))
+ (k6(i+1)*C(i,5)*C(i,6));
R_BD = (k1(i+1)*C(i,2)*C(i,1))-(k2(i+1)*C(i,3)*C(i,6))+(k3(i+1)*C(i,3)*C(i,1))-
(k4(i+1)*C(i,4)*C(i,6))+(k5(i+1)*C(i,4)*C(i,1))-(k6(i+1)*C(i,5)*C(i,6));
R_GL = (k5(i+1)*C(i,4)*C(i,1)) - (k6(i+1)*C(i,5)*C(i,6));
R_MetOH = -(k1(i+1)*C(i,2)*C(i,1))+(k2(i+1)*C(i,3)*C(i,6))-
(k3(i+1)*C(i,3)*C(i,1))+(k4(i+1)*C(i,4)*C(i,6))-
(k5(i+1)*C(i,4)*C(i,1))+(k6(i+1)*C(i,5)*C(i,6));
%We store the molar gain of each component in an R matrix:
R(i,1) = R_MetOH; R(i,2) = R_TG; R(i,3) = R_DG; R(i,4) = R_MG;
R(i,5) = R_GL; R(i,6) = R_BD;
M(i,:) = R(i,:)*vr; %The change in molar holdup of each component saved in a vector
Msum(i,1) = sum(M(i,:));
end
%The order of compounds is as before: MetOH/TG/DG/MG/GL/BD
                                    %    1  2  3  4  5  6


%% Molar balances in the column (the states)
dHxdt = zeros(Ntrays+2,5);
dHdt = zeros(Ntrays+2,1);

% Column
i = 2:Ntrays_react+1;
dHdt(i,1) = L(i-1,1) - L(i,1) + V(i,1) - V(i-1,1) + Msum(i-1);

i = Ntrays_react+2:Ntrays+1;
dHdt(i,1) = L(i-1) - L(i) + V(i,1) - V(i-1,1);

%Correction for the feed:
dHdt(2,1) = dHdt(2,1) + F0;


%The molar holdup composition balance for the feed tray:
for j = 1:5;
    for i = 2
        dHxdt(i,j) = ((F0*x_in(j,1)) + (V(i,1)*y(i,j)) + L(i-1,1)*xL(i-1,j) - (V(i-
1,1)*y(i-1,j)) - (L(i,1)*xL(i,j)) + M(i-1,j));
    end
end

%The molar holdup composition balance for the two other reactive trays:
for j = 1:5;
    for i = 3:Ntrays_react+1
```

```
        dHxdt(i,j) = (V(i,1)*y(i,j)) + (L(i-1,1)*xL(i-1,j) - (V(i-1,1)*y(i-1,j)) -
(L(i,1)*xL(i,j)) + M(i-1,j));
    end
end

%The molar holdup composition balance for the non-reactive trays:
 for j = 1:5;
     for i = Ntrays_react+2:Ntrays+1;
        dHxdt(i,j) = (V(i,1)*y(i,j)) + (L(i-1,1)*xL(i-1,j)) - (V(i-1,1)*y(i-1,j)) -
(L(i,1)*xL(i,j));
     end
 end

%Reboiler (assumed to be an equilibrium stage)
i = Ntrays+2;
dHdt(i,1) = L(Ntrays+1,1) - V(Ntrays+1,1) - B;

j=1:5;
dHxdt(i,j)= (L(Ntrays+1,1)*xL(Ntrays+1,j) - V(Ntrays+1,1)*y(Ntrays+2,j) -
B*xL(Ntrays+2,j));

%Total condenser (not an equilibrium stage)
i = 1;
dHdt(i,1) = V(1,1) - L(1,1) - D;

j = 1:5;
dHxdt(i,j)= V(1,1)*y(i,j) - L(1,1)*xL(i,j) - D*xL(i,j);

%Computing the derivative for the mole fractions from d(Mx) = x dM + M dx
dxdt=(dHxdt - (xL.*(dHdt*ones(1,5)))./(HL*ones(1,5));

dxdtout = reshape(dxdt,(Ntrays+2)*5,1);
dxdtout = [dxdtout; dHdt];


block.Derivatives.Data = dxdtout;
```

B. Simulink Model

A print of the Simulink model is given here. The dynamic version was submitted electronically.

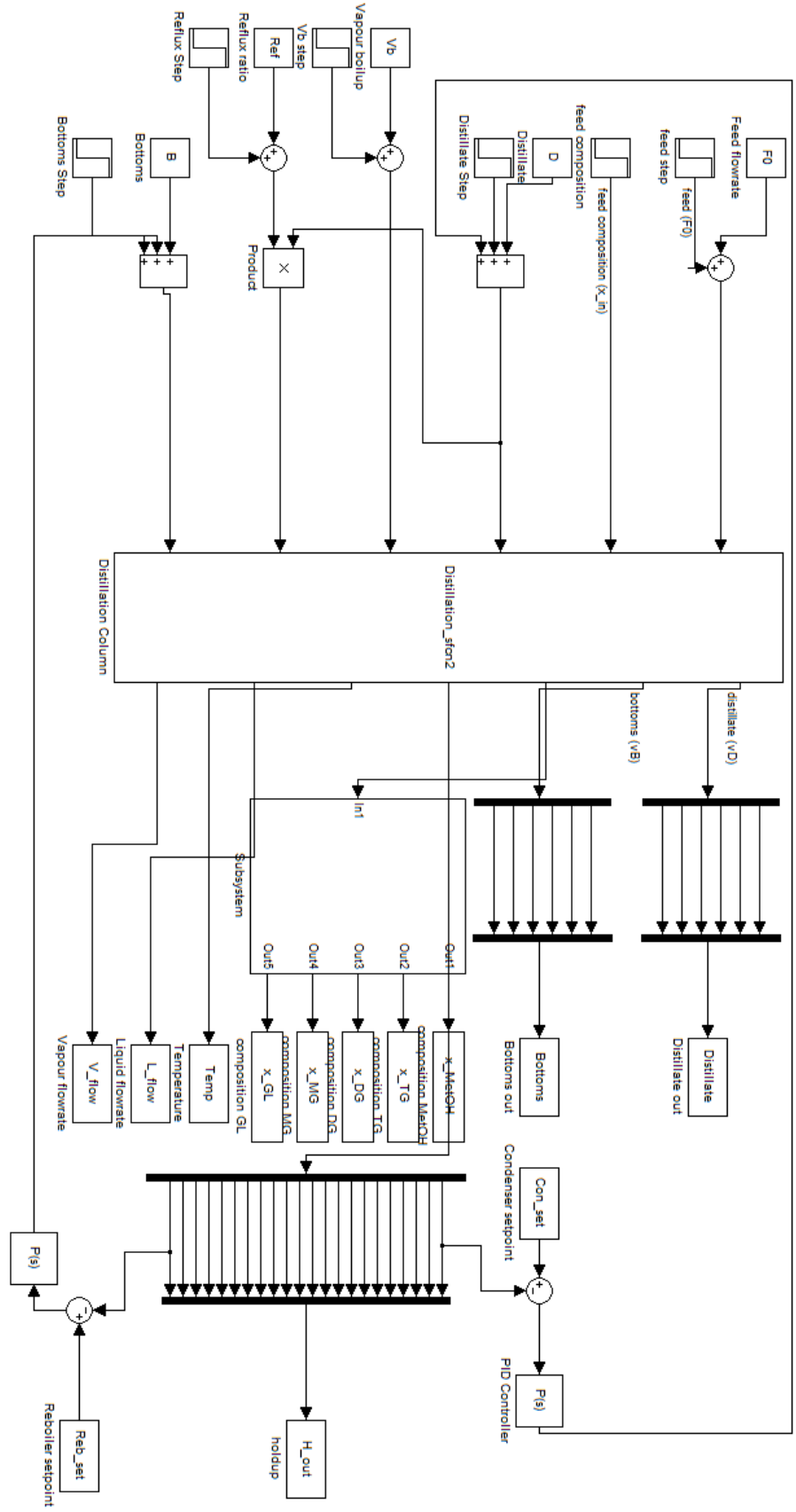

C. Estimation of Critical Temperatures and Pressures

The critical temperatures and pressures were estimated according to the Joback method as described on page 12 of "The Properties of Gases and Liquids" [22].

C.1 The Joback Method

The Joback method is a group contribution method. This means that it will estimate critical properties of pure compounds based on the functional groups in the molecule. The Joback method allows for fast and easy estimations of critical properties, but it does not have the greatest accuracy for all compounds. The Joback method is one of the recommended methods for application when a reliable value for the boiling point is available [22].

The equations for the critical temperatures and pressures are given below as equations C.1 and C.2 [22].

$$T_c = T_b[0.584 + 0.965 \sum \Delta T - (\sum \Delta T)^2]^{-1} \quad \text{(C.1)}$$

$$P_c = (0.113 + 0.0032 N_A - \sum \Delta P)^{-2} \quad \text{(C.2)}$$

The parameters ΔT and ΔP are the functional group contribution values to the critical temperature and pressures and are given in Table C.1 below, while N_A is the number of atoms present in the molecule. Table C.1 also contains the number of said functional groups that are present in the monolinolein and dilinolein molecules. The chemical structure of monolinolein and dilinolein is visualised in Figure C.1.

Table C.1: Group contributions to P_c and T_c

Functional Group	T_c	P_c	Number of groups DG	Number of groups MG
$-CH_3$	0.0141	−0.0012	2	1
$-CH_2-$	0.0189	0	26	14
$-CH=$	0.0129	−0.0006	8	4
$-COO-$	0.0481	0.0005	2	1
$-CH<$	0.0164	0.0020	1	1
$-OH$	0.0741	0.0112	1	2

The calculations for ΔT and ΔP for MG and DG are shown below:

$$\Delta T[DG] = 2(0.0141) + 26(0.0189) + 8(0.0129) + 2(0.0481) + 0.0164 + 0.0741 = 0.8095$$

$$\Delta T[MG] = 0.0141 + 14(0.0189) + 4(0.0129) + 0.0481 + 0.0164 + 2(0.0741) = 0.5430$$

$$\Delta P[DG] = 2(-0.0012) + 8(-0.0006) + 2(0.0005) + 0.0020 + 0.0112 = 0.0070$$

$$\Delta P[MG] = -0.0012 + 4(-0.0006) + 0.0005 + 0.0020 + 2(0.0112) = 0.0213$$

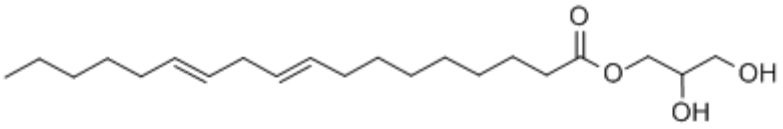

MONOLINOLEIN

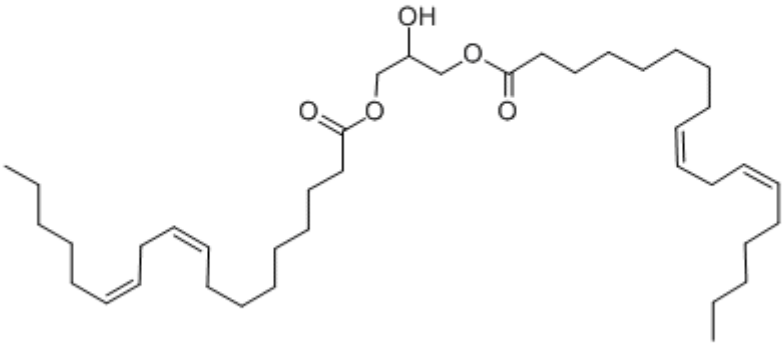

DILINOLEIN

Figure C.1: The chemical structures of monolinolein [33] and dilinolein[34]

By applying equations C.1 and C.2 as well as the boiling points of DG and MG that were given in Table 3.2, the critical temperatures and pressures were estimated:

$$T_c[DG] = 942.57[0.584 + 0.965(0.8095) - (0.8095)^2]^{-1} = 1327.79K$$

$$T_c[MG] = 758.20[0.584 + 0.965(0.5430) - (0.5430)^2]^{-1} = 932.43K$$

$$P_c[DG] = (0.113 + 0.0032(112) - 0.0070)^{-2} = 4.6368bar$$

$$P_c[MG] = (0.113 + 0.0032(63) - 0.0213)^{-2} = 11.625bar$$

D. Estimation of Vapour Pressure Equations

The vapour pressure equations for monolinolein and dilinolein were estimated according to a modified Clausius-Clapeyron equation, the Riedel equation. The Riedel method for estimating vapour pressures is fairly accurate for pure compounds, but validity is lower when approaching lower temperatures and pressures. The equation is given below as number D.1, and gives the vapour pressure in MPa[35].

$$\ln(P_r) = A - \frac{B}{T_r} + C \cdot \ln(T_r) + D \cdot T_r^6 \quad \text{(D.1)}$$

Here the first three terms represent the integration of the Clausius-Clapeyron equation, while the last term was added by Riedel to reduce inaccuracies. The reduced pressure and reduced temperature is defined as shown in equations D.2 and D.3 [35].

$$P_r = \frac{P^*}{P_c} \qquad \text{(D.2)}$$

$$T_r = \frac{T}{T_c} \qquad \text{(D.3)}$$

By algebraic manipulation of equations D.2 and D.3 one can get an expression for P^* and T. These can be substituted into equation D.1 and then a vapour pressure equation dependent on the system temperature has been derived:

$$P^* = \exp\left[A - \frac{B}{T_r} + C\ln(T_r) + DT_r^6\right] \qquad \text{(D.4)}$$

The constants of equation D.4 are defined as [35]:

$$A = -35Q, \quad B = -36Q, \quad C = 42Q + \alpha_c, \quad D = -Q$$

To calculate the constants, one needs to obtain the variables α_c and Q. The constant Q is an empirical parameter found from correlations in vapour pressure experimental data. To obtain α_c, and in turn Q, one must first equate T_{br}, P_{br} and ψ_b:

$$T_{br} = \frac{T_b}{T_c} \qquad \text{(D.5)}$$

$$P_{br} = \frac{0.101325}{P_c} \qquad \text{(D.6)}$$

$$\psi_b = -35 + \frac{36}{T_{br}} + 42 \cdot \ln(T_{br}) - T_{br}^6 \qquad \text{(D.7)}$$

$$\alpha_c = \frac{K_1 K_2 \psi_b - \ln(P_{br})}{K_1 \psi_b - \ln(T_{br})} \qquad \text{(D.8)}$$

$$Q = K_1(K_2 - \alpha_c) \qquad \text{(D.9)}$$

The values of K_1 and K_2 are 0.0838 and 3.758 respectively. Once all of these constants are derived, one can substitute them into equation D.4 and get an expression for the vapour pressure.

D.1 The Calculation – Dilinolein

The first step was to calculate the values for T_{br} and P_{br}:

$$T_{br} = \frac{942.6}{1327.8} = 0.7099, \qquad P_{br} = \frac{0.101325}{0.46368} = 0.21852$$

Next the values for ψ_b, α_c and Q were computed:

$$\psi_b = -35 + \frac{36}{0.7099} + 42 \cdot \ln(0.7099) - 0.7099^6 = 1.19287$$

$$\alpha_c = \frac{0.0838 \cdot 3.758 \cdot 1.19287 - \ln(0.21852)}{0.0838 \cdot 1.19287 - \ln(0.7099)} = 4.2850$$

$$Q = 0.0838(3.758 - 4.2850) = -0.04416$$

The α_c and Q were then used to calculate the constants A, B, C and D:

$$A = -35(-0.04416) = 1.5457, \qquad B = -36(-0.04416) = 1.5898$$

$$C = 42(-0.04416) + 4.2850 = 2.4303, \qquad D = -(-0.04416) = 0.04416$$

Inserted into equation D.4 along with the critical temperature, the vapour pressure equation for dilinolein is:

$$P_{DG}^* = \exp\left[1.5457 - \frac{1.5898(1327.84)}{T} + 2.4303(\ln(T) - \ln(1327.84)) + \frac{0.04416 \cdot T^6}{1327.84^6}\right]$$

$$P_{DG}^* = \exp\left[-15.9313 - \frac{2111.0}{T} + 2.4303\ln(T) + (8.0567 \cdot 10^{-21} \cdot T^6)\right]$$

D.2 The Calculation – Monolinolein

The first step was to calculate the values for T_{br} and P_{br}:

$$T_{br} = \frac{758.2}{932.43} = 0.8131, \qquad P_{br} = \frac{0.101325}{1.1625} = 0.087161$$

Next the values for ψ_b, α_c and Q were computed:

$$\psi_b = -35 + \frac{36}{0.8131} + 42 \cdot \ln(0.8131) - 0.8131^6 = 0.29617$$

$$\alpha_c = \frac{0.0838 \cdot 3.758 \cdot 0.29617 - \ln(0.087161)}{0.0838 \cdot 0.29617 - \ln(0.8131)} = 10.9324$$

$$Q = 0.0838(3.758 - 10.9324) = -0.60121$$

The α_c and Q were then used to calculate the constants A, B, C and D:

$$A = -35(-0.60121) = 21.0425, \qquad B = -36(-0.60121) = 21.6436$$

$$C = 42(-0.60121) + 10.9324 = -14.3184, \qquad D = -(-0.60121) = 0.60121$$

Inserted into equation D.4 along with the critical temperature, the vapour pressure equation for dilinolein is:

$$P_{MG}^{*} = \exp\left[21.0425 - \frac{21.6436(932.43)}{T} - 14.3184(\ln(T) - \ln(932.43)) + \frac{0.60121 \cdot T^{6}}{932.43^{6}}\right]$$

$$P_{MG}^{*} = \exp\left[118.9488 - \frac{20181.142}{T} - 14.3184\ln(T) + (9.1481 \cdot 10^{-19} \cdot T^{6})\right]$$

E. Francis Weir Calculation

The Francis weir parameters were calculated roughly according to the method described in the Fluid Dynamics section of the report. Because the feed is introduced on the first stage, the parameters are designed for the part of the column below the feed.

E.1 Parameters

The parameters needed for the calculation are listed below, with some comments as to why they were chosen.

```
T = 373.15;                    % Temperature [K]
```

The temperature was set based on the temperature achieved in the simulation by Simasatitkul et al. [1] .

```
X = [0.75 0.15 0.10];          % The composition of three main components
[wt%]
Mw = [294.47 32 92.094];       % The molecular weights [kg/kmol]
```

The calculation was only based on the three main components, methanol, methyl linoleate and glycerol in the following order: [BD MetOH GL]. The composition of the components was derived from the simulation results by Simasatitkul et al. for the middle section of the column.

```
P1 = [4.25 352420 25.588];   % Vapour pressures [Pa]
Psat = P1*9.869*10^(-6);     % Vapour pressures [atm]
```

The vapour pressures were calculated in the DIPPR Project 801 database at 373.15K, and converted to atm.

```
R = 0.082057;                % Gas constant [m3*atm/K*kmol]
rho_v = sum((Psat.*Mw)/(R*T));  % The vapour density [kg/m3]
rho1 = [2.827 22.16 13.12]; % The liquid density [kmol/m3]
rho_l = sum(rho1.*Mw.*X);    % The liquid density [kg/m3]
Vw = (430*Mw(1,2))/3600;     % The vapour flowrate [kg/s]
Lw = (sum(675*X.*Mw))/3600; % The liquid flowrate [kg/s]
```

The equation for the vapour density uses the ideal gas equation. The vapour phase is assumed to consist only of methanol.

E.2 Design Calculations

The following calculations were made in the design of the trays:

```
Flv = (Lw/Vw)*sqrt(rho_v/rho_l) % Equals 0.75
```

The F_{LV} was calculated by applying equation X, and is used to find a value for K_1 by reading off Figure 11.27 in Chemical Engineering Design by Coulson and Richardson[27]. This gives:

```
K1 = 0.034;
```

The parameter K_1 is then applied to equation 4.2 to find the flooding velocity, and then the actual velocity which equals 0.85 of the flooding velocity.

```
uf = K1*sqrt((rho_l-rho_v)/rho_v)  % Flooding vapour velocity [m/s] =0.5192
u_real = 0.85*uf                   % real vapour velocity [m/s] =0.4413
```

Next, the vapour velocity was used to find the volumetric velocity:

```
vm = sum(Vw./rho_v)                % volumetric flowrate [m3/s] =1.0512
```

The volumetric vapour velocity could then be used to find the required area and the diameter:

```
An = vm/u_real                     % Net area required [m] =2.3819
```

```
Ac = An/0.88                          % Cross-section area [m] =2.7068
D = sqrt((Ac*4)/pi)                   % Column diameter [m] =1.8564
lw = 0.77*D                           % Weir length [m] = 1.4295
```

Here, the net area was found, which was used to find the cross-section of the column, assuming that the downflow is approximately 12%. Next, the diameter of the column was calculated, and from there one can calculate the length of the weir as it is known that the weir is approximately 77% of the column diameter.

The rest of the Francis weir calculations were implemented in the dynamic model, as it is directly influenced by changes in the liquid holdup.

E.3 Dynamic Model

In the dynamic model, the Francis weir equation was implemented:

```
% Applying Francis weir for the liquid flowrates
how = ones(Ntrays,1); Lw = ones(Ntrays,1);
for i = 1:Ntrays
    %Calculation of height over weir [m]:
      how(i,1) = (HL(i+1,1)-
(pi*hw*rho_l(i+1,1)*0.88*(Dc/2)^2))/(pi*0.88*(Dc/2)^2);
      if how(i,1) <0
          %Ensures no negative flowrates within column
          Lw(i+1,1) = 0;
          L(i+1,1) = 0;
      else
          %Francis weir [kg/s]
          Lw(i+1,1) = ((how(i,1)*10^3)/750)^1.5*rho_L(i+1,1)*lw;
          %Liquid flowrate [kmol/h]
          L(i+1,1) = (Lw(i+1,1)*3600)/sum(XX(i+1,:).*Mw);
      end
end
```

The height over weir is calculated according to the mass balance 4.5 with no foaming, while the liquid mass flow is calculated from the Francis weir formula. The molar liquid flowrate is the end product and is used in the molar balances.

F. Bubble and Dew Point Estimations

This is an overview of the calculations for the bubble and dew point temperatures and enthalpies, so that the liquid feed fraction could be estimated.

F.1 Parameters

The necessary parameters for the calculation are given below:

```
A_met = 82.718;
B_met = -6.9045*10^3;
C_met = -8.8622;
D_met = 7.4664*10^-6;
E_met = 2;

A_TG = 234.71;
B_TG = -3.4699*10^4;
C_TG = -27.25;
D_TG = 1.5475*10^-18;
E_TG = 6;
```

This represents the parameters for the vapour pressure equations derived from the DIPPR project 801 database for methanol and trilinolein in the feed.

F.2 Bubble Point

Method - Temperature

The bubble point was estimated using an iterative method applying Raoult's law:

1. An initial value for the temperature was set.
2. The vapour pressure was calculated for all components present.
3. The total pressure was calculated, with the liquid fractions being equal to the composition of the feed.
4. The difference between the actual pressure and the calculated pressure was estimated
5. If the difference is too large, re-estimate T and continue steps 2-4 until convergence has been achieved.

Calculation - Temperature

This is a copy of the Matlab script written. Comments have been made where necessary.

```
x_met = 6/7;
x_TG = 1/7;
```

The molar fractions of the feed are stated. The iteration for the bubble point temperature is given in a for-loop:

```
for T = 323.15:0.001:1000
    Temp(i,1) = T;
    P_met(i,1) = 9.869*(10^-6)*exp(A_met + (B_met/T) + (C_met*log(T)) +
(D_met*T^E_met));
    P_TG(i,1) = 9.869*(10^-6)*exp(A_TG + (B_TG/T) + (C_TG*log(T)) +
(D_TG*T^E_TG));
    P(i,1) = (x_met*P_met(i,1))+(x_TG*P_TG(i,1));
    e(i,1) = 1-P(i,1); %The error from the actual pressure of 1 atm
    if e(i,1) <= 0.0001 && e(i,1) >= 0
        disp([T])
        break
    else i = i+1;
        T = T + 0.01;
```

```
    end
end
```

Here the first temperature to satisfy the demands with an error of 0.0001 is recorded and stored. The bubble point temperature obtained is 341.65K

Enthalpy

The heats of formation and heats of vaporisation for methanol and trilinolein are given in Table F.1 below. The values are from the DIPPR 801 database. An intermediate value was used for the liquid heat capacity.

Table F.1: The heats of formation and heat of condensation for methanol and trilinolein

	MetOH [kJ/kmol]	TG [kJ/kmol]
$\Delta H_f[298.15]$	$-239\ 100$	$-1\ 748\ 000$
$-\Delta H_{vap}[298.15]$	$-37\ 460$	$-221\ 070$
$Cp_l[298.15-341.65]$	86.158	1 745.050

The calculations are shown below:

$$\Delta H_{MetOH}[298.15-341.65]=\sum Cp\cdot\Delta T=3\ 747.873$$

$$\Delta H_{MetOH}[341.65]=\Delta H_f-\Delta H_{vap}+\sum Cp\cdot\Delta T=-272\ 812.127$$

$$\Delta H_{TG}[298.15-341.65]=\sum Cp\cdot\Delta T=75\ 909.675$$

$$\Delta H_{TG}[341.65]=\Delta H_f-\Delta H_{vap}+\sum Cp\cdot\Delta T=-1\ 893\ 160.325$$

Combining the enthalpies with the molar fractions, the enthalpy at the bubble point is calculated:

$$\Delta H[341.65]=x_{MetOH}\cdot\Delta H_{MetOH}+x_{TG}\cdot\Delta H_{TG}=-504\ 290.441\ kJ/kmol$$

F.3 Dew point

Method - Temperature

The dew point was estimated by applying an iterative method with basis in Raoults law, similar to the method listed for bubble point calculations. But for this case, it is the vapour phase composition that is equal to the feed composition and it is equation F.1 that should converge to zero.

$$P_T=\frac{1}{\sum_{i=1}^{NC}(y_i/P_i)} \qquad \text{(F.1)}$$

Calculation - Temperature

In the dew point calculation, the vapour phase should have the feed composition. Hence the vapour phase composition is given by:

```
y_met = 6/7;
y_TG = 1/7;
```

The vapour phase composition of the feed is stated. The iteration for the dew point temperature is similar to the bubble point iteration and is given below:

```
for T = 323.15:0.001:1000
    Temp(i,1) = T;
    P_met(i,1) = 9.869*(10^-6)*exp(A_met + (B_met/T) + (C_met*log(T)) +
(D_met*T^E_met));
    P_TG(i,1) = 9.869*(10^-6)*exp(A_TG + (B_TG/T) + (C_TG*log(T)) +
(D_TG*T^E_TG));
    P(i,1) = 1/((y_met/P_met(i,1))+(y_TG/P_TG(i,1)));
    e(i,1) = 1-P(i,1); %The error from the actual pressure of 1 atm
    if e(i,1) <= 0.0001 && e(i,1) >= 0
        disp([T])
        break
    else i = i+1;
        T = T + 0.001;
    end
end
```

The error here is also 0.0001 in the total pressure. The estimated dew point temperature was 799.75K.

Enthalpy

The heat of formation from Table F.1 can also be used here, the heat of vaporization is not necessary as all the feed will be in the vapour phase at the dew point.

The heat capacity is temperature dependent; hence Table F.2 and Table F.3 were created which calculate the heat capacity from 298.15K to the dewpoint temperature with a temperature interval of 50K for methanol and trilinolein respectively.

Table F.2: Calculation of the ideal vapour heat capacity for methanol

Temperature [K]	Cp [kJ]	Cp for the interval	$Cp \cdot \Delta T$ [kJ]
298.15	44.007		
348.15	47.580	45.794	2 289.675
398.15	51.568	49.574	2 478.700
448.15	55.644	53.606	2 680.300
498.15	59.625	57.635	2 881.725
548.15	63.434	61.530	3 076.475
598.15	67.045	65.240	3 261.975
648.15	70.459	68.752	3 437.600
698.15	73.683	72.071	3 603.550
748.15	76.726	75.205	3 760.225
799.75	79.686	78.206	4 035.430

$$\Delta H_{MetOH}[298.15 - 799.75] = \sum Cp \cdot \Delta T = 31\,505.655$$

$$\Delta H_{MetOH}[799.75] = \Delta H_f + \sum Cp \cdot \Delta T = -207\,594.345$$

Table F.3: Calculation of the heat capacity for trilinolein

Temperature [K]	Cp [kJ]	Cp for the interval	$Cp \cdot \Delta T$ [kJ]
298.15	1 270.800		
348.15	1 439.400	1 355.100	67 755.000
398.15	1 608.500	1 523.950	76 197.500
448.15	1 766.800	1 687.650	84 382.500
498.15	1 910.400	1 838.600	91 930.000
548.15	2 039.100	1 974.750	98 737.500
598.15	2 154.500	2 096.800	104 840.000
648.15	2 258.700	2 206.600	110 330.000
698.15	2 353.800	2 306.250	115 312.500
748.15	2 441.200	2 397.500	119 875.000
799.75	2 524.900	2 483.050	128 125.380

$$\Delta H_{TG}[298.15 - 799.75] = \sum Cp \cdot \Delta T = 997\,485.380$$

$$\Delta H_{TG}[799.75] = \Delta H_f + \sum Cp \cdot \Delta T = -750\,514.620$$

Combining the enthalpies with the molar fractions, the enthalpy at the dew point is calculated:

$$\Delta H[799.75] = x_{MetOH} \cdot \Delta H_{MetOH} + x_{TG} \cdot \Delta H_{TG} = -285\,154.385\ kJ/kmol$$

F.4 Feed Liquid Fraction

The enthalpy at the feed temperature was calculated by the same method as in the bubble point calculation and is equal to -510 434.445 kJ/kmol. The calculation of the feed liquid fraction is then straight forward implementation of equation 4.8:

$$q = \frac{H_V - H_F}{H_V - H_L} = \frac{-285154 + 510434}{-285154 + 504290} = 1.028$$

The feed liquid fraction will vary with the feed temperature, but only the feed enthalpy will change. Table F.4 gives an overview of the different values for q at different temperatures

Table F.4: The feed liquid fraction at different temperatures

Temperature [K]	ΔH_f [kJ/kmol]	Feed liquid fraction
298.15	-518 347.143	1.064
303.15	-516 784.055	1.057
313.15	-513 619.222	1.043
323.15	-510 434.445	1.028
333.15	-507 129.294	1.013
343.15	-503 800.078	0.998
353.15	-500 411.269	0.982

G. DAE System

This appendix contains the Matlab scripts for the DAE estimation for the temperature. This is split into two scripts: the main code (main_scriptDAE.m) and the s-function (reactive_distDAE.m). These are given below:

G.1 The Main Matlab Script

This is the main code for running the simulation of the DAE system.

```
% Written by Emilie Ø. Houge
% The main code for running the DAE system for temperature iteration by
% Raoult's law.

%clc, close all, clear all

temporary = ones(132,1);
temporary1 = zeros(22,1);
m_matrix = diag([temporary;temporary1]);
options = odeset('mass', m_matrix);

load('steadystate_DAE.mat');
y0_0 = steadystate_DAE(1,:);
T0 = 373.15*ones(1,22);
y0 = [y0_0 T0];
tic
[t, y] = ode15s(@reactive_distDAE, [0 100], y0, options);
toc

x = y(end,1:110);
H = y(end,111:132);
T = y(end,133:154);

x_comp = reshape(x,22,5);
```

G.2 The Function

The function contains all data, equations and specifications required for the model.

```
function F = reactive_distDAE(t,Y)
% This file is a modified version of Sigurds flash.m file

% I. Data:
Ntrays = 20; %The number of trays
NC = 6;      %The number of compounds
R = 8.314472*10^(-3);       %Gas constant [kJ/K*mol]
Mw = [32.0 879.3844 616.95 354.52 92.094 294.47]; %Molecular weights [kg/kmol]
Ntrays_react = 10;           %Number of reactive trays
q = 1.0280;                 %Feed liquid fraction
F = [300 50 0 0 0 0];       %Feed [kmol/h]
F0 = sum(F);                %Total feed [kmol/h]
x_in = F/F0;                %Molar fractions
Vb = 430;                   %Vapour boilup
Dc = 1.8564;                        %Diameter of column [m]
lw = 1.4295;                        %Length of weir [m]
hw = 0.20;                  %Heigth of weir [m]
D = 105;                 %Distillate [kmol/h]
B = 244.9;                 %Bottoms, [kmol/h]
Ref = 3*D;                  %Reflux ratio

% Parameters for the vapour pressure equations:
A_met = 82.718; B_met = -6.9045*10^3; C_met = -8.8622; D_met = 7.4664*10^-6; E_met
= 2;
A_TG = 234.71; B_TG = -3.4699*10^4; C_TG = -27.25; D_TG = 1.5475*10^-18; E_TG = 6;
```

```
A_DG = -15.931; B_DG = -2111.0; C_DG = 2.4303; D_DG = 8.0567*10^-21; E_DG = 6;
A_MG = 118.95; B_MG = -2.0181*10^4; C_MG = -14.32; D_MG = 9.148*10^-19; E_MG = 6;
A_GL = 99.986; B_GL = -1.3808*10^4; C_GL = -10.088; D_GL = 3.5712*10^-19; E_GL = 6;
A_BD = 105.47; B_BD = -1.4531*10^4; C_BD = -10.986; D_BD = 2.5735*10^-18; E_BD = 6;

% II. Extract present value of states
x = Y(1:(Ntrays+2)*(NC-1),1);   % Compositions of compounds 1-5 on each tray
H = Y(111:132,1);               % Molar holdup on each tray [kmol]
T = Y(133:154,1);               % Temperature on each tray [K]
xL = reshape(x,Ntrays+2,NC-1);  % Reshaping the  compositions
HL = reshape(H,Ntrays+2,1);     % Reshaping the molar holdups
TL = reshape(T,Ntrays+2,1);     % Reshaping the temperature

% IIIa. Intermediate calculations
%Liquid and vapour molar flows:
V = ones(Ntrays+1,1);  %V is a vector of the molar vapor flows in the column
V(1,1) = D + Ref;      %From a molar balance over the top of the column
L = ones(Ntrays+1,1);  %L is a vector of the different trays in the column.
L(1,1) = Ref;          %The first liquid molar flow is equal to the reflux.

XX = zeros(Ntrays+2,NC);  x_BD = zeros(Ntrays+2,1);
for i = 1:Ntrays+2
    x_BD(i,1) = 1 - sum(xL(i,:));
    XX(i,:) = [xL(i,:) x_BD(i,1)];
end

%% Calculation of density
% Initialising sizes
rho_MetOH = ones(Ntrays+2,1); rho_TG = ones(Ntrays+2,1); rho_GL = ones(Ntrays+2,1);
rho_BD = ones(Ntrays+2,1); rho_DG = ones(Ntrays+2,1); rho_MG = ones(Ntrays+2,1);
rho = [rho_MetOH rho_TG rho_DG rho_MG rho_GL rho_BD];
rho_l = ones(Ntrays+2,1); rho_L = ones(Ntrays+2,1); x_wt = zeros(Ntrays+2,NC);

% The constants
Ar_met = 2.3267; Br_met = 0.27073; Cr_met = 512.5; Dr_met = 0.24713;
Ar_TG = 0.026085; Br_TG = 0.14259; Cr_TG = 934.6; Dr_TG = 0.28571;
Ar_GL = 0.92382; Br_GL = 0.24386; Cr_GL = 850; Dr_GL = 0.22114;
Ar_BD = 0.20469; Br_BD = 0.23737; Cr_BD = 767.4; Dr_BD = 0.28571;

for i = 1:Ntrays+2
    %Density [kmol/m3]
      rho_MetOH(i,1) = Ar_met/(Br_met^(1+(1-(T(i,1)/Cr_met))^Dr_met));
      rho_TG(i,1) = Ar_TG/(Br_TG^(1+(1-(T(i,1)/Cr_TG))^Dr_TG));
      rho_GL(i,1) = Ar_GL/(Br_GL^(1+(1-(T(i,1)/Cr_GL))^Dr_GL));
      rho_BD(i,1) = Ar_BD/(Br_BD^(1+(1-(T(i,1)/Cr_BD))^Dr_BD));
      rho_DG(i,1) = ((2/3)*rho_TG(i,1)) + ((1/3)*rho_BD(i,1));
      rho_MG(i,1) = ((1/3)*rho_TG(i,1)) + ((2/3)*rho_BD(i,1));
      rho(i,:) = [rho_MetOH(i,1) rho_TG(i,1) rho_DG(i,1) rho_MG(i,1) rho_GL(i,1)
rho_BD(i,1)];
      %A common liquid density for the tray [kmol/m3]
      rho_l(i,1) = sum(rho(i,:).*XX(i,:));
      %Weight fraction
      x_wt(i,:) = (XX(i,:)*HL(i,1).*Mw)/sum(XX(i,:)*HL(i,1).*Mw);
      %A common liquid density for the tray [kg/m3]
      rho_L(i,1) = sum(rho(i,:).*Mw.*x_wt(i,:));
end


% Applying Francis weir for the liquid flowrates
% Initializing sizes
V = ones(Ntrays+1,1);  %V is a vector of the molar vapor flows in the column
L = ones(Ntrays+1,1);  %L is a vector of the different trays in the column.

% Applying Francis weir for the liquid flowrates
how = ones(Ntrays,1); Lw = ones(Ntrays,1);
for i = 1:Ntrays
      how(i,1) = (HL(i+1,1)-(pi*hw*rho_l(i+1,1)*0.88*(Dc/2)^2))/(pi*0.88*(Dc/2)^2);
%Calculation of how
```

```
      Lw(i+1,1) = ((how(i,1)*10^3)/750)^1.5*rho_L(i+1,1)*lw;    %Francis weir
[kg/s]
      L(i+1,1) = (Lw(i+1,1)*3600)/sum(XX(i+1,:).*Mw);           %Liquid flow
[kmol/h]
end

% Vapour flowrates
V(Ntrays+1,1) = Vb;  %The vapour from the last tray is equal to the vapour boilup

% Assuming constant molar overflow for vapour flowrates
for i = 2:Ntrays
    V(i,1) = V(Ntrays+1,1);
end

% Correction for the feed:
V(1,1) = V(2,1) + ((1-q)*F0);% The vapour flowrate over the feed has been reduced
by qF0

% Molar balances over the top and the bottom:
L(1,1) = Ref;                % The first liquid molar flow is equal to the reflux.

% VLE
y = zeros(Ntrays+2,5);
P = ones(Ntrays+2,1);
for j = 1:Ntrays+2
P_met = 9.869*(10^-6)*exp(A_met + (B_met/TL(j,1)) + (C_met*log(TL(j,1))) +
(D_met*TL(j,1)^E_met));
P_TG = 9.869*(10^-6)*exp(A_TG + (B_TG/TL(j,1)) + (C_TG*log(TL(j,1))) +
(D_TG*TL(j,1)^E_TG));
P_DG = 9.869*exp(A_DG + (B_DG/TL(j,1)) + (C_DG*log(TL(j,1))) +
(D_DG*TL(j,1)^E_DG));
P_MG = 9.869*exp(A_MG + (B_MG/TL(j,1)) + (C_MG*log(TL(j,1))) +
(D_MG*TL(j,1)^E_MG));
P_GL = 9.869*(10^-6)*exp(A_GL + (B_GL/TL(j,1)) + (C_GL*log(TL(j,1))) +
(D_GL*TL(j,1)^E_GL));
P_BD = 9.869*(10^-6)*exp(A_BD + (B_BD/TL(j,1)) + (C_BD*log(TL(j,1))) +
(D_BD*TL(j,1)^E_BD));
x_BD = 1 - sum(xL(j,:));
P(j,1) =
(xL(j,1)*P_met)+(xL(j,2)*P_TG)+(xL(j,3)*P_DG)+(xL(j,4)*P_MG)+(xL(j,5)*P_GL)+(x_BD*P
_BD);
y(j,1) = (P_met*xL(j,1))/P(j,1);
y(j,2) = (P_TG*xL(j,2))/P(j,1);
y(j,3) = (P_DG*xL(j,3))/P(j,1);
y(j,4) = (P_MG*xL(j,4))/P(j,1);
y(j,5) = (P_GL*xL(j,5))/P(j,1);
end

%% Kinetics
%The sizes of the kinetic constants:
k1 = ones(Ntrays+2,1); k2 = ones(Ntrays+2,1); k3 = ones(Ntrays+2,1);
k4 = ones(Ntrays+2,1); k5 = ones(Ntrays+2,1); k6 = ones(Ntrays+2,1);

for i = 1:Ntrays+2
%Kinetic data for the reaction
%rate constants [m3/kmol*h]
k1(i) = 3.9*3600*(10^7)*exp(-54.9987/(R*TL(i,1)));
k2(i) = 5.78*3600*(10^5)*exp(-41.5555/(R*TL(i,1)));
k3(i) = 5.906*3600*(10^12)*exp(-83.0942/(R*TL(i,1)));
k4(i) = 9.888*3600*(10^9)*exp(-61.2496/(R*TL(i,1)));
k5(i) = 5.335*3600*(10^3)*exp(-26.8655/(R*TL(i,1)));
k6(i) = 2.1*3600*(10^4)*exp(-40.1162/(R*TL(i,1)));
end

%We need to convert the molar input to concentrations in order to calculate
%the reaction outputs:
C = zeros(Ntrays_react,6); %Creates a matrix with reactive trays as rows and a
column for each compound
```

```
R = zeros(Ntrays_react,6);
M = zeros(size(C));
Msum = zeros(Ntrays_react,1);
for i = 1:Ntrays_react
   x_BD = 1 - sum(xL(i+1,:));   %Finding the fraction of biodiesel from mass
balance
   XXL = [xL(i+1,:) x_BD];      %The liquid fraction vector includig the 6th state
   vH = HL(i+1,1)*XXL;          %molar holdup vector
   vr = sum(vH./rho(i+1));      %volume holdup
   C(i,:) = vH/vr;              %concentration of each component
%The reactions. R is the gain/loss in moles/h
R_TG = -(k1(i+1)*C(i,2)*C(i,1)) + (k2(i+1)*C(i,3)*C(i,6));
R_DG = (k1(i+1)*C(i,2)*C(i,1)) - (k2(i+1)*C(i,3)*C(i,6)) - (k3(i+1)*C(i,3)*C(i,1))
+ (k4(i+1)*C(i,4)*C(i,6));
R_MG = (k3(i+1)*C(i,3)*C(i,1)) - (k4(i+1)*C(i,4)*C(i,6)) - (k5(i+1)*C(i,4)*C(i,1))
+ (k6(i+1)*C(i,5)*C(i,6));
R_BD = (k1(i+1)*C(i,2)*C(i,1))-(k2(i+1)*C(i,3)*C(i,6))+(k3(i+1)*C(i,3)*C(i,1))-
(k4(i+1)*C(i,4)*C(i,6))+(k5(i+1)*C(i,4)*C(i,1))-(k6(i+1)*C(i,5)*C(i,6));
R_GL = (k5(i+1)*C(i,4)*C(i,1)) - (k6(i+1)*C(i,5)*C(i,6));
R_MetOH = -(k1(i+1)*C(i,2)*C(i,1))+(k2(i+1)*C(i,3)*C(i,6))-
(k3(i+1)*C(i,3)*C(i,1))+(k4(i+1)*C(i,4)*C(i,6))-
(k5(i+1)*C(i,4)*C(i,1))+(k6(i+1)*C(i,5)*C(i,6));
%We store the molar gain of each component in an R matrix:
R(i,1) = R_MetOH; R(i,2) = R_TG; R(i,3) = R_DG; R(i,4) = R_MG;
R(i,5) = R_GL; R(i,6) = R_BD;
M(i,:) = R(i,:)*vr; %The change in molar holdup of each component saved in a vector
Msum(i,1) = sum(M(i,:));
end

% IIIb. Evaluate right hand side of DAE-set: M dy/dt = f(y)
f1 = zeros(Ntrays+2,5);
f2 = zeros(Ntrays+2,1);

% Column
i = 2:Ntrays_react+1;
f2(i,1) = L(i-1,1) - L(i,1) + V(i,1) - V(i-1,1) + Msum(i-1);

i = Ntrays_react+2:Ntrays+1;
f2(i,1) = L(i-1) - L(i) + V(i,1) - V(i-1,1);

%Correction for the feed:
f2(2,1) = f2(2,1) + F0;


%The molar holdup composition balance for the feed tray:
for j = 1:5;
    for i = 2
        f1(i,j) = ((F0*x_in(1,j)) + (V(i,1)*y(i,j)) + L(i-1,1)*xL(i-1,j) - (V(i-
1,1)*y(i-1,j)) - (L(i,1)*xL(i,j)) + M(i-1,j));
    end
end

%The molar holdup composition balance for the two other reactive trays:
for j = 1:5;
    for i = 3:Ntrays_react+1
        f1(i,j) = (V(i,1)*y(i,j)) + (L(i-1,1)*xL(i-1,j) - (V(i-1,1)*y(i-1,j)) -
(L(i,1)*xL(i,j)) + M(i-1,j));
    end
end

%The molar holdup composition balance for the non-reactive trays:
 for j = 1:5;
     for i = Ntrays_react+2:Ntrays+1;
        f1(i,j) = (V(i,1)*y(i,j)) + (L(i-1,1)*xL(i-1,j)) - (V(i-1,1)*y(i-1,j)) -
(L(i,1)*xL(i,j));
     end
 end
```

```
%Reboiler (assumed to be an equilibrium stage)
i = Ntrays+2;
f2(i,1) = L(Ntrays+1,1) - V(Ntrays+1,1) - B;

j=1:5;
f1(i,j)= (L(Ntrays+1,1)*xL(Ntrays+1,j) - V(Ntrays+1,1)*y(Ntrays+2,j) -
B*xL(Ntrays+2,j));

%Total condenser (not an equilibrium stage)
i = 1;
f2(i,1) = V(1,1) - Ref - D;

j = 1:5;
f1(i,j)= V(1,1)*y(i,j) - L(1,1)*xL(i,j) - D*xL(i,j);

%For the algebraic equation for the temperature:
f3 = zeros(Ntrays+2,1);
for i = 1:Ntrays+2
    f3(i,1) = 1 - P(i,1);    %=0, the psat-equations are dependent on temperature
end

f1_1 =(f1 - (xL.*(f2*ones(1,5)))./(HL*ones(1,5));
f1 = reshape(f1_1,(Ntrays+2)*(NC-1),1);

F = [f1; f2; f3];
```